Properties of Low Dimensional Dynamical Systems in the Large

Carles Simó

Dept. Matemàtica Aplicada i Anàlisi, UB

carles@maia.ub.es

Long Time Semiclassical Evolution

Wolfgang Pauli Institute

Vienna, 070108-12

A problem

Consider a **totally elliptic** fixed point of an **autonomous Hamiltonian system or a symplectic map**. It is **linearly stable** if the eigenvalues are simple.

Questions:

a) What about **non linear stability**? In general not true for **3 or more degrees of freedom (DOF)**. There is no way to avoid **Arnol'd diffusion** (except in simple cases when some **Dirichlet-like theorem** applies). But perhaps one can talk about **practical stability** in some sense (mild diffusion in very long time intervals).

b) Up to which distance **there is stability in some sense**? Which **objects** appear at the **stability boundaries** (perhaps in a **weak or practical** sense).

c) How do the results depend on **parameters**?

These are **global** questions. Require use of **analytics** and **numerics**.

Furthermore

1) How can be do **simulations**, specially in the case of **differential equations** and which is the effect of **round off** errors in long term simulations?

2) Which kind of **indicators** can be used to check the **regular or chaotic** behaviour of the dynamics?

3) How can be compute the **skeleton** of the dynamics, i.e., the **relevant invariant objects**, such as fixed points, periodic orbits, invariant tori, invariant manifolds, homo/hetero-clinic objects?

4) Which objects sit at the **boundaries of stability** or of **practical stability**?

5) How to convert a careful **numerical evidence** into a **rigorous proof**?

6) Which kind of **paradigmatic models** can help to understand different pieces of the dynamics?

The lectures are based on several papers and/or ongoing work.

The collaboration of many persons like H. Broer, P. Cincotta, E. Fontich, V. Galiot, V. Gelfreich, C. Giordano, G. Gómez, S. Gonchenko, T. Kapela, R. Martínez, J.M. Mondelo, A. Neishtadt, D. Treschev, A. Vasiliev, A. Vieiro, R. Vitolo, etc, is warmly acknowledged.

A toy problem: the Hénon map

Any quadratic area preserving map can be reduced to

$$\begin{pmatrix} x \\ y \end{pmatrix} \to \begin{pmatrix} x_1 \\ y_1 \end{pmatrix} = \begin{pmatrix} c(1-x^2)+2x+y \\ -x \end{pmatrix} \qquad x, y, c \in \mathbb{R}.$$

With this normalisation **fixed points** at H$= (-1, 1)$ and E$= (1, -1)$.

Last one **elliptic** if $c \in [0, 2]$. A **Normal Form** analysis proves **non linear stability** if $c \in (0, 2) \setminus \{1.5\}$.

Case $c < 0$ reduced to previous case via $(x, y, c) \longrightarrow (-x, -y, -c)$.

Let us consider first c small. The map can be approximated by a **flow**. The symplectic change

$$\begin{pmatrix} x \\ y \end{pmatrix} = \frac{1}{\sqrt{2}} \begin{pmatrix} q+p \\ q-p \end{pmatrix}$$

allows to write

$$\begin{pmatrix} q \\ p \end{pmatrix} \longrightarrow \begin{pmatrix} q + \hat{c}(1 - \frac{1}{2}(q+p)^2) \\ p + 2q + \hat{c}(1 - \frac{1}{2}(q+p)^2) \end{pmatrix},$$

where $\hat{c} = c/\sqrt{2}$. Let $d = \sqrt{\hat{c}}$ and introduce (u, v) by $p = u$, $q = dv$, giving the **close to the identity map**

$$\begin{pmatrix} u \\ v \end{pmatrix} \longrightarrow \begin{pmatrix} u + 2dv + O(d^2) \\ v + d(1 - \frac{1}{2}u^2) + O(d^2). \end{pmatrix}$$

A map of the form $(u, v)^t \to (u + df(u, v) + O(d^2), v + dg(u, v) + O(d^2)^t)$ can be approximated by the **time d flow** of $(\dot{u}, \dot{v})^t = (f, g)^t$, giving now

$$\dot{u} = 2v, \qquad \dot{v} = 1 - \frac{1}{2}u^2,$$

which comes from the Hamiltonian $K(u, v) = v^2 - u + \frac{1}{6}u^3$. The level $K = \frac{2}{3}\sqrt{2}$ containing the hyperbolic point $u = -\sqrt{2}, v = 0$ corresponds to a **separatrix**, enclosing the elliptic point $u = \sqrt{2}, v = 0$. The **splitting** for the manifolds of the map is **exponentially small in d.** Also **invariant curves** of the map exist at an **exponentially small** distance of the manifolds.

Sketch of the ideas to prove these facts. Based on **complex extensions of $W^{u,s}$** and suitable parametrizations and on the **separatrix and standard maps**.

The **area enclosed** by the separatrix of the flow is finite. Going back to (x, y) it must be $O(\sqrt{c})$, as we shall check.

A **global stability** criterion: Points which do not escape to infinity.

Relevant comment: In this toy problem (equivalent to a Poincaré map of a 2DOF Hamiltonian) there are domains of **true stability** due to **KAM theorem**.

Let us scan the domain $[-1, 2.1] \times [-1, 2.1]$ with step size 0.001 and keep the non escaping points. All points outside this domain escape. Different checks are done concerning criteria, number of iterates, etc.

We display **global results** and a **movie**.

General comments on the results. How to **explain** all the features?

We remark that the Hénon map is a **local model** for many islands of APM (**Area Preserving Maps**). Hence, the features found appear in some part of the phase space of **most APM**.

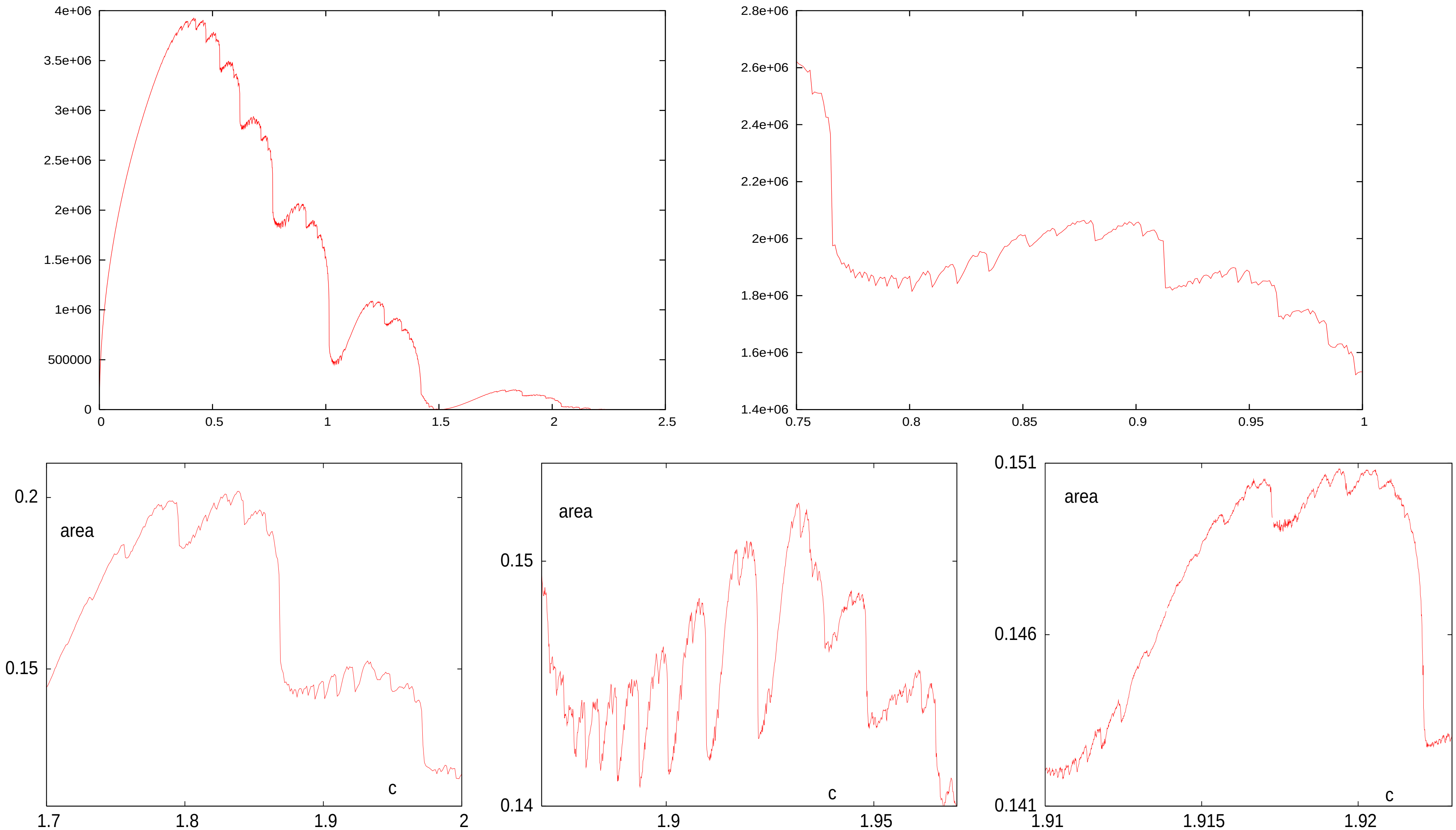

Statistics of results and some details.

The **ultimate boundaries** to confine motion are the **invariant manifolds** of H. But for some escaping points it can be necessary **a large number of iterations** to reach a small nbd of H.

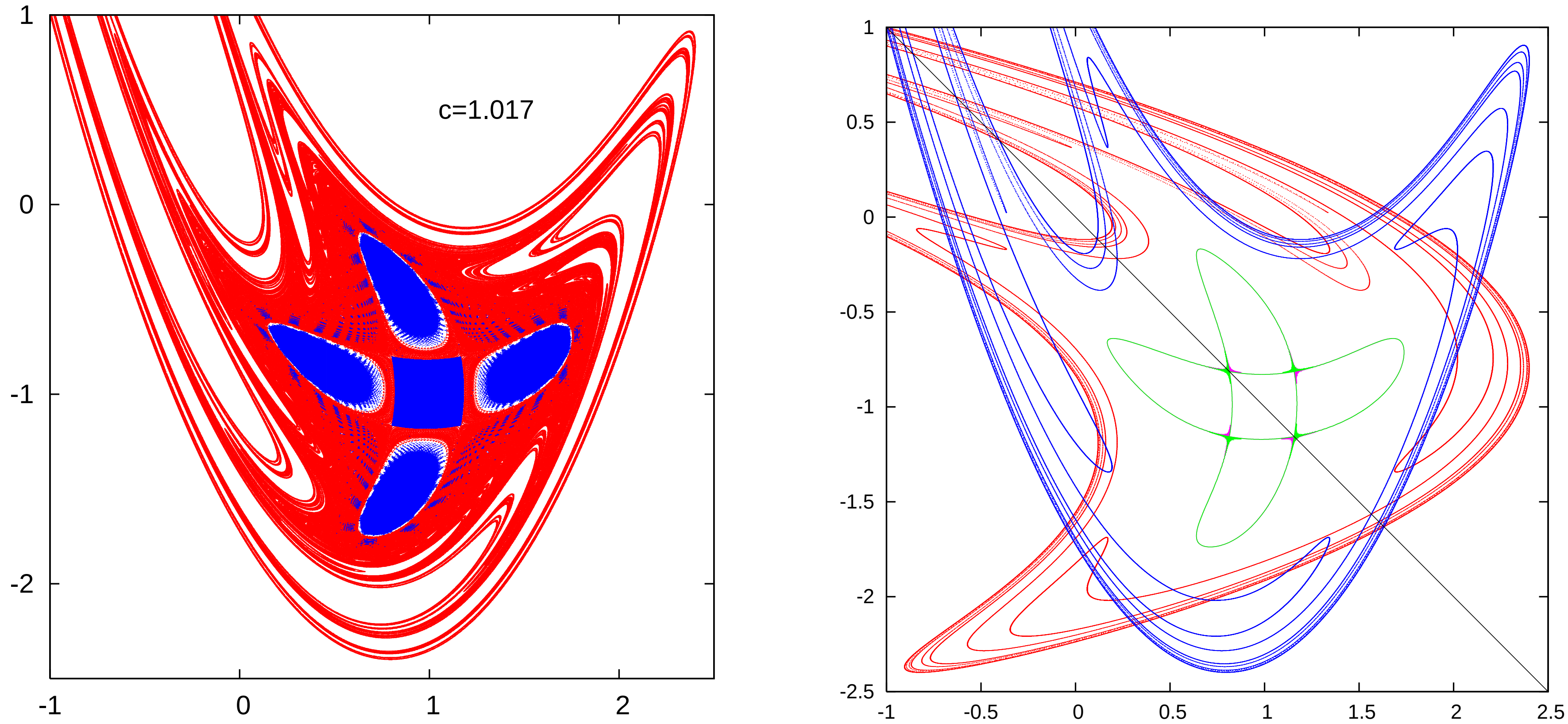

Left: Points in W_H^s (red) and non escaping (blue) for $c = 1.017$. Right: Manifolds of H (W_H^s in blue, W_H^u in red) and of the hyperbolic period-4 orbit (in magenta and green, resp.) for $c = 1.015$. Note that red and green finally connect.

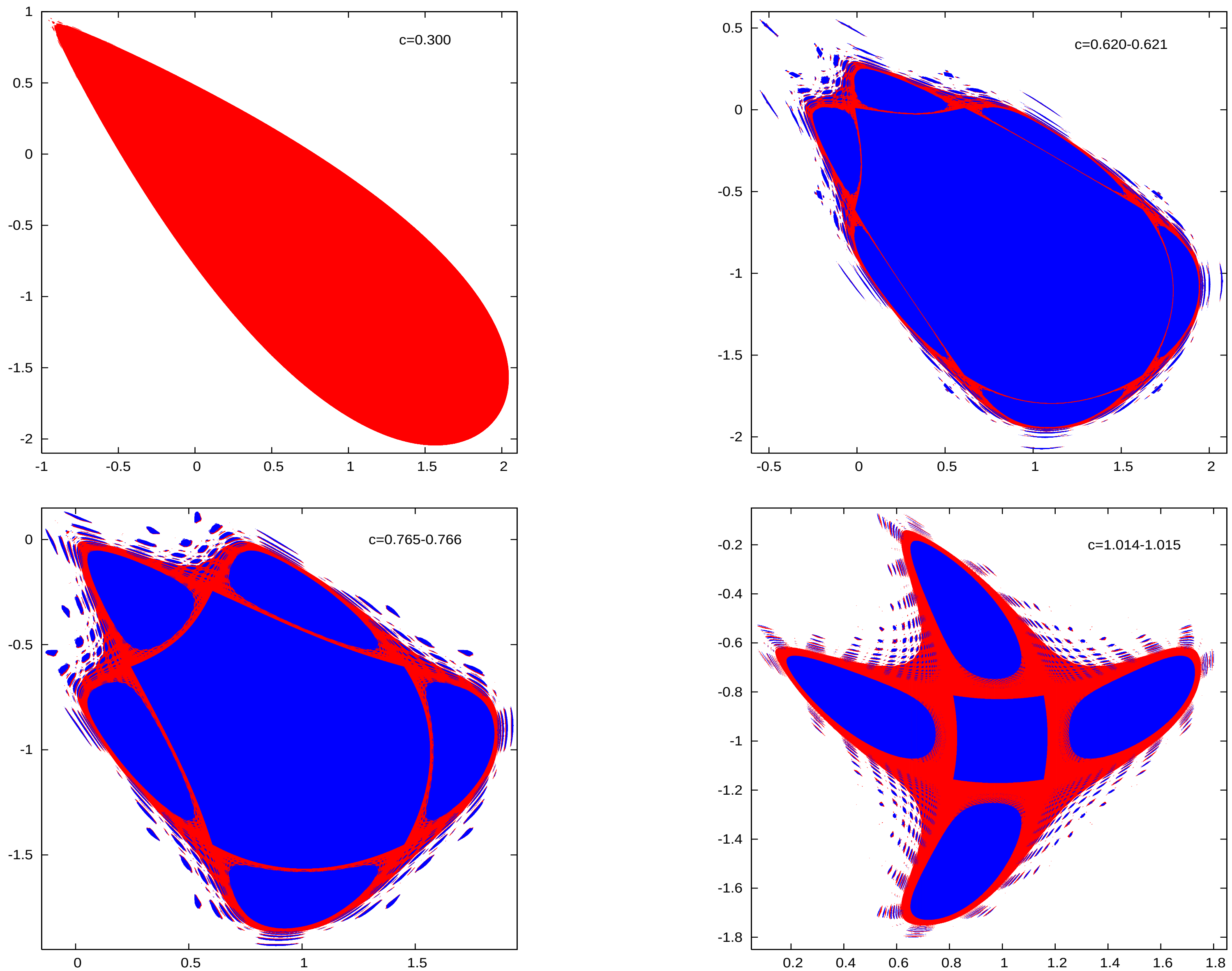

Examples of the results for selected c and transitions.

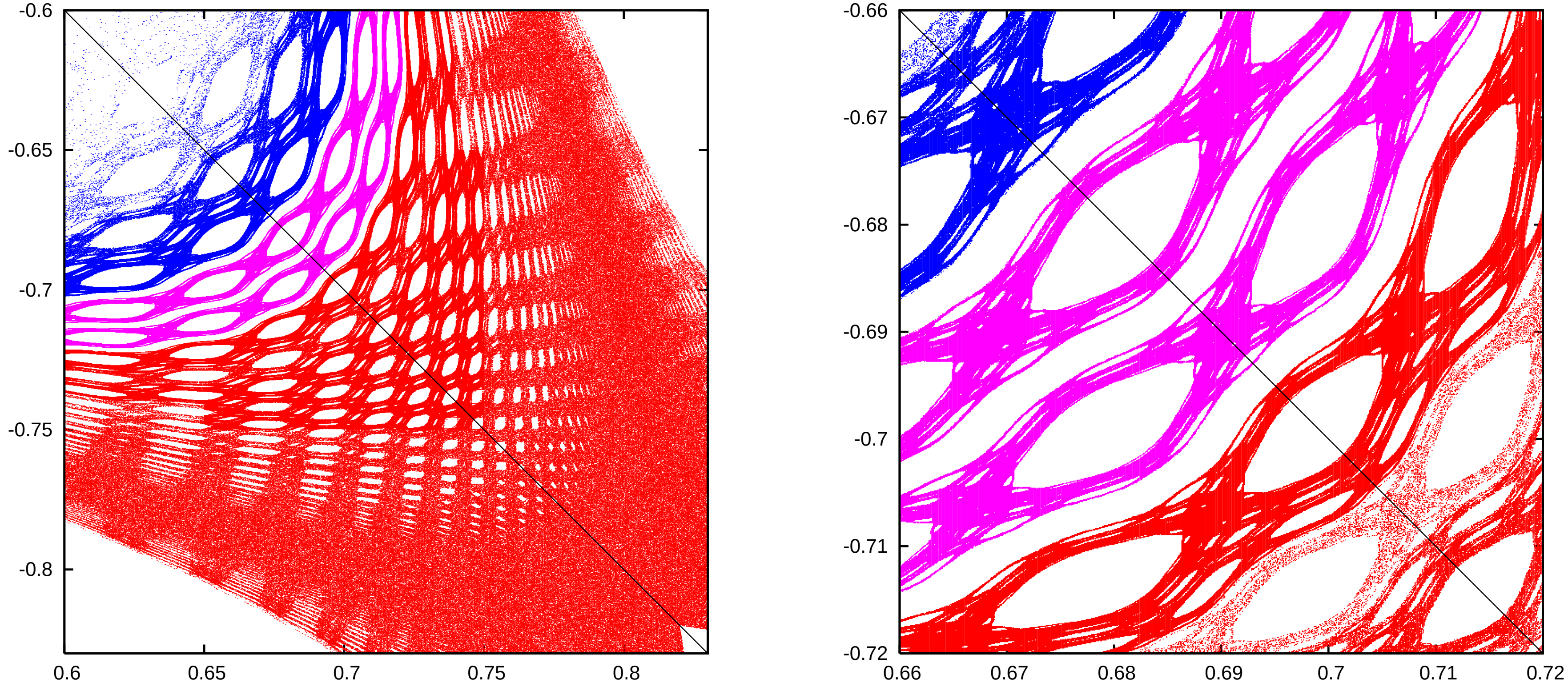

Magnifications of a region close to $y = -x$ for $c = 1.0141$. Points in red, blue, correspond to **single orbits**. Points in magenta correspond to **two orbits**, one in each domain. One can see the **negative** of the **islands**. Only points in blue escape, but **for** $c = 1.0142$ **all these points escape**. For $c = 1.0141$ there are **three gaps** candidate to contain **invariant (rotational) curves**.

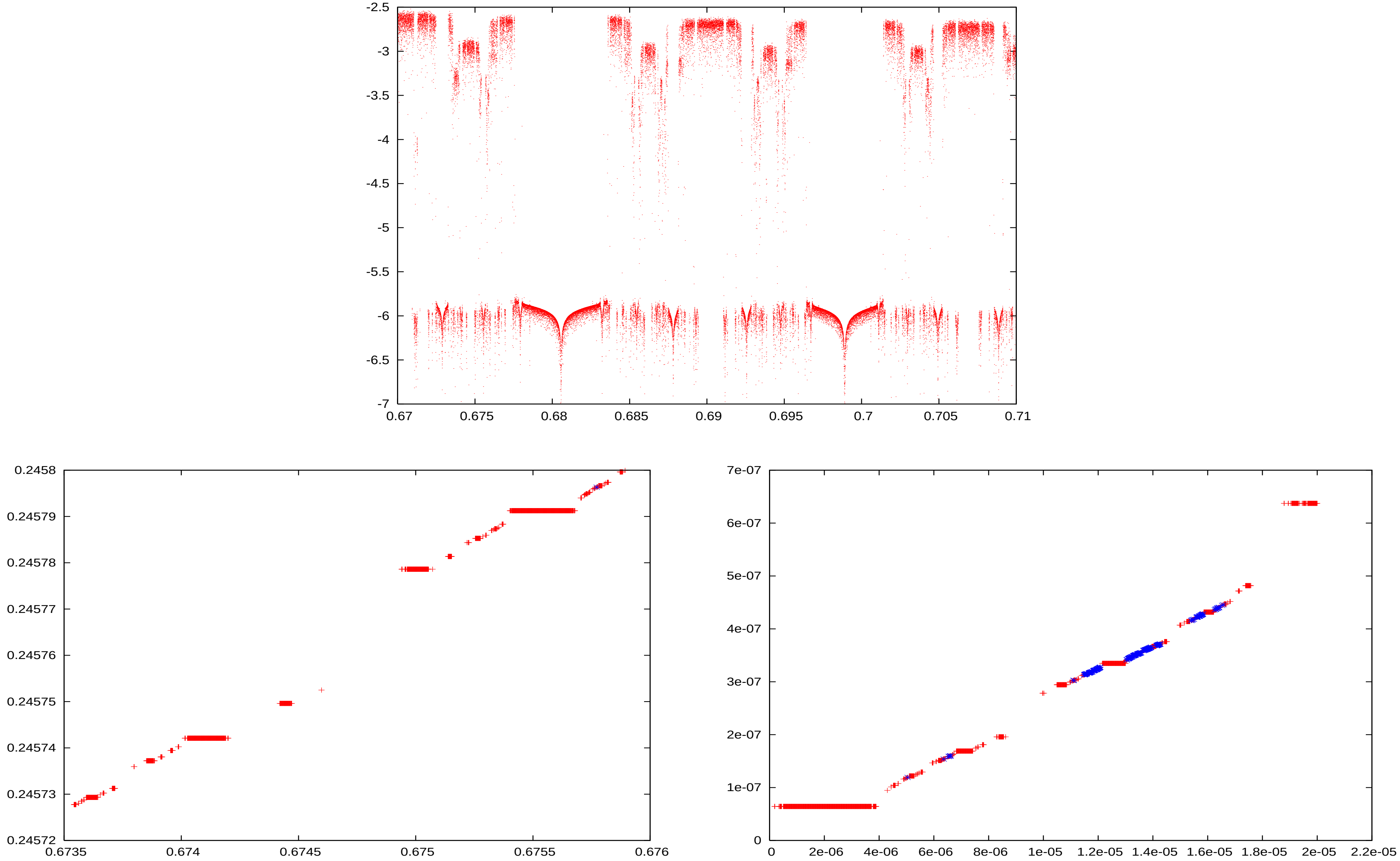

Lyapunov exponent (in $\log_{10}$) and **rotation number** for selected decreasing intervals. In {bfblue candidates to **invariant curve** (not well approximated by rationals with denominator less than 10^7).

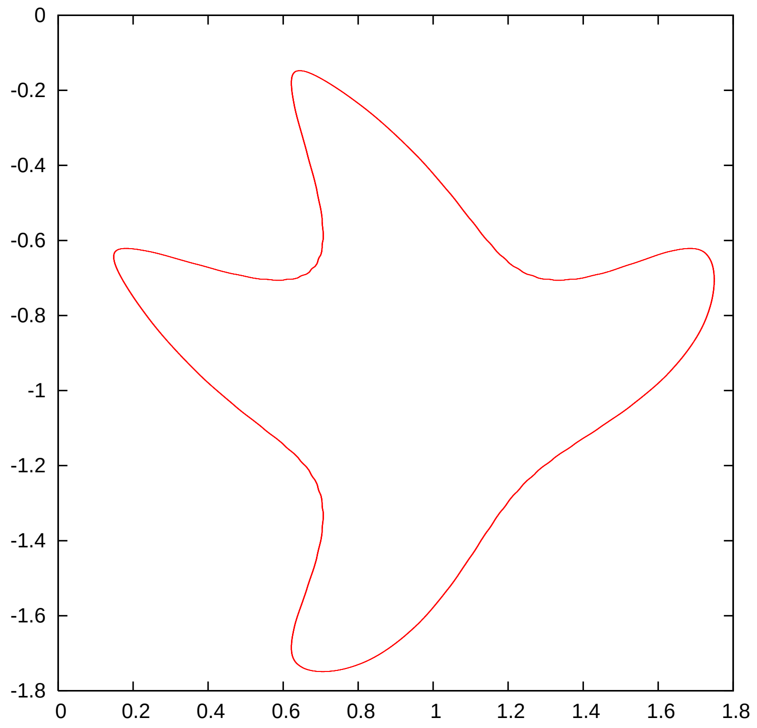

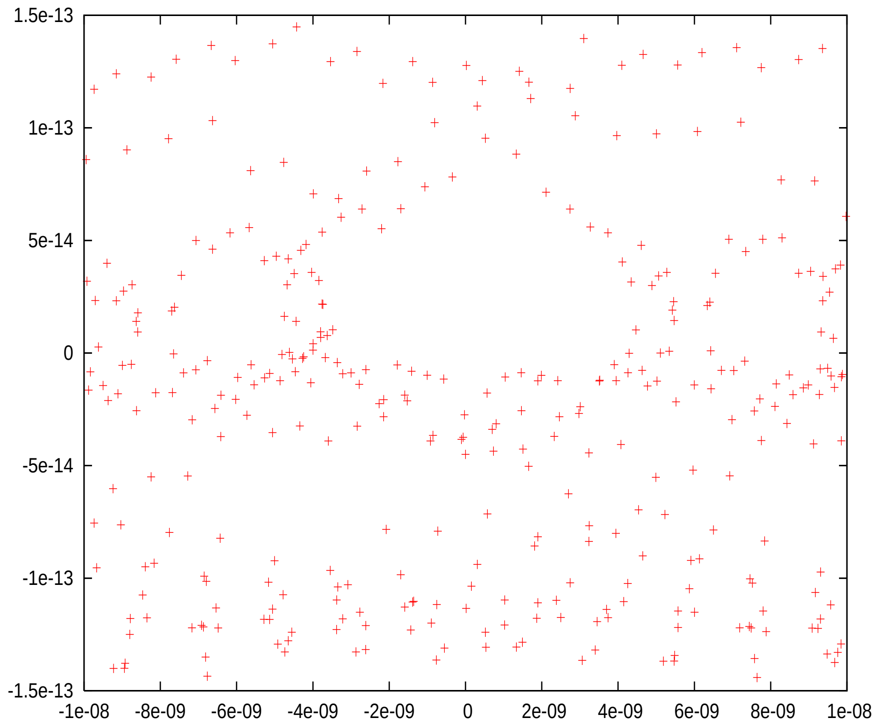

Left: What seems to be an **invariant curve** for $c = 1.0141$ passing through $x_0 = -y_0 = 0.6757666$. Right: Iterates with $|x - x_0| < 10^{-8}$ among the first 10^{10} iterates, after the **affinity** $(x, y) \mapsto (x - x_0, y - x + 2x_0)$ and **subtracting a quadratic fit**. **Width** of the cloud of points: 3×10^{-13}.

Discussion on **averaging** and **exponentially small splitting** .

Separatrix maps

Consider the behaviour near a **broken separatrix**, either single loop or figure 8. A model can be derived by considering **passage close to the saddle** and **gluing maps**. The central plot also shows the **simplest type of periodic orbit** with points in the **lobes** created by the splitting.

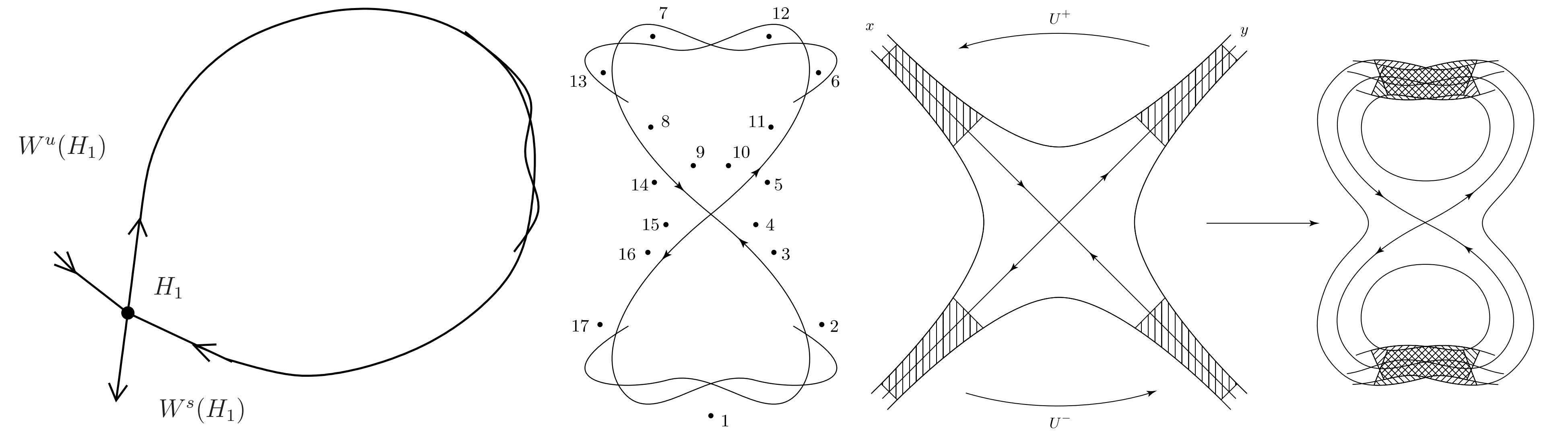

In the case of central plot we introduce **action-angle** coordinates (q, p, σ) where q is taken mod 1 to cover a fundamental domain (e.g., from the left end of the lobe containing 7 to the right one of lobe containing 12). Variable p measures distance to the stable manifold and σ is a sign to denote upper or lower part.

A **general separatrix map**, which is an $O(\varepsilon)$ of an integrable map having dominant eigenvalue λ at H, has the form

$$S_\varepsilon \begin{pmatrix} q \\ p \\ \sigma \end{pmatrix} = \begin{pmatrix} Q \\ P \\ \rho \end{pmatrix} = \begin{pmatrix} q + \frac{1+O(\varepsilon)}{\log\lambda}\Big[\log(\varepsilon\alpha_\sigma^{-2}) + \log|P|\Big] \\ p + \alpha_\sigma^2 \nu_\sigma (q - \log\alpha_\sigma / \log\lambda) + O(\varepsilon) \\ \sigma \,\mathrm{sign}\, P \end{pmatrix},$$

where the ν_σ express the shape of the splitting in these coordinates.

As a simple case (and in some sense typical) we have the **Chirikov separatrix map**, which scaling p by the size of the splitting and identifying lower and upper parts reads

$$SM \begin{pmatrix} x \\ y \end{pmatrix} = \begin{pmatrix} \bar{x} \\ \bar{y} \end{pmatrix} = \begin{pmatrix} x + a + b\log(|\bar{y}|) \\ y + \sin(2\pi x) \end{pmatrix}.$$

For b large SM looks quite chaotic near $y = 0$. It seems that **inside the lobes** the dynamics is **fully chaotic**, but it has been proved that the fraction of ε (in log scale) for which there are stable islands inside the lobe, tends to **a positive constant** if $\varepsilon \to 0$. Sketch of proof.

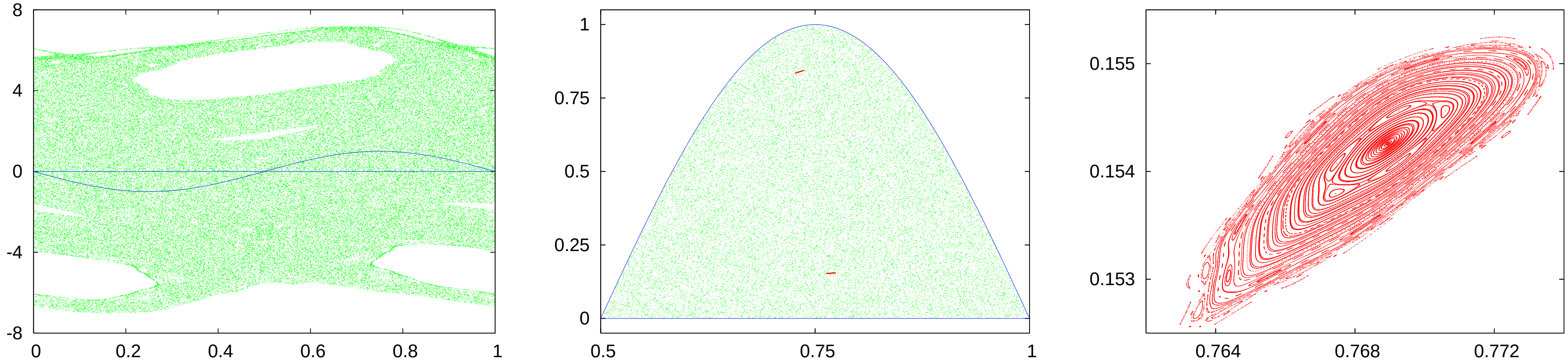

Left: 10^5 first iterates of $A = (0.01, 0.01)$ under SM for $(a, b) = (0.407, 1)$, showing also $W^{u,s}$. Middle: magnification using first 10^6 iterates and the right lobe. **Stable islands** in red. Right: magnification of an island.

Now assume $y = y_0 + r$ with $y_0 >> 1, r = O(1)$. Expanding $\log(y_0 + \bar{r}) = \log(y_0) + \bar{r}/y_0 + O(1/y_0^2)$

$$\begin{pmatrix} x \\ r \end{pmatrix} = \begin{pmatrix} \bar{x} \\ \bar{r} \end{pmatrix} \approx \begin{pmatrix} x + \hat{a} + \frac{b}{y_0}\bar{r} \\ r + \sin(2\pi x) \end{pmatrix},$$

where $\hat{a} = a + b\log(y_0)$. Using $z = \hat{a} + r$ and skipping $O(y_0^{-2}$ we obtain

$$\begin{pmatrix} x \\ z \end{pmatrix} = \begin{pmatrix} \bar{x} \\ \bar{z} \end{pmatrix} = \begin{pmatrix} x + \varepsilon\bar{z} \\ z + \sin(2\pi x) \end{pmatrix},$$

where $\varepsilon = \frac{b}{y_0}$, a usual form of the **classical standard map**. It has **invariant rotational curves** (i.e., graphs of $z = g(x)$) if $\varepsilon < \varepsilon_G \approx 0.9716/(2\pi)$, the so-called **Greene's critical value**.

This implies invariant curves for SM provided $\frac{b}{y_0} < \varepsilon_G$. We recall that y is measured in units of the size of the splitting (i.e., **invariant rotational curves exist at exponentially small distance of the invariant manifolds**).

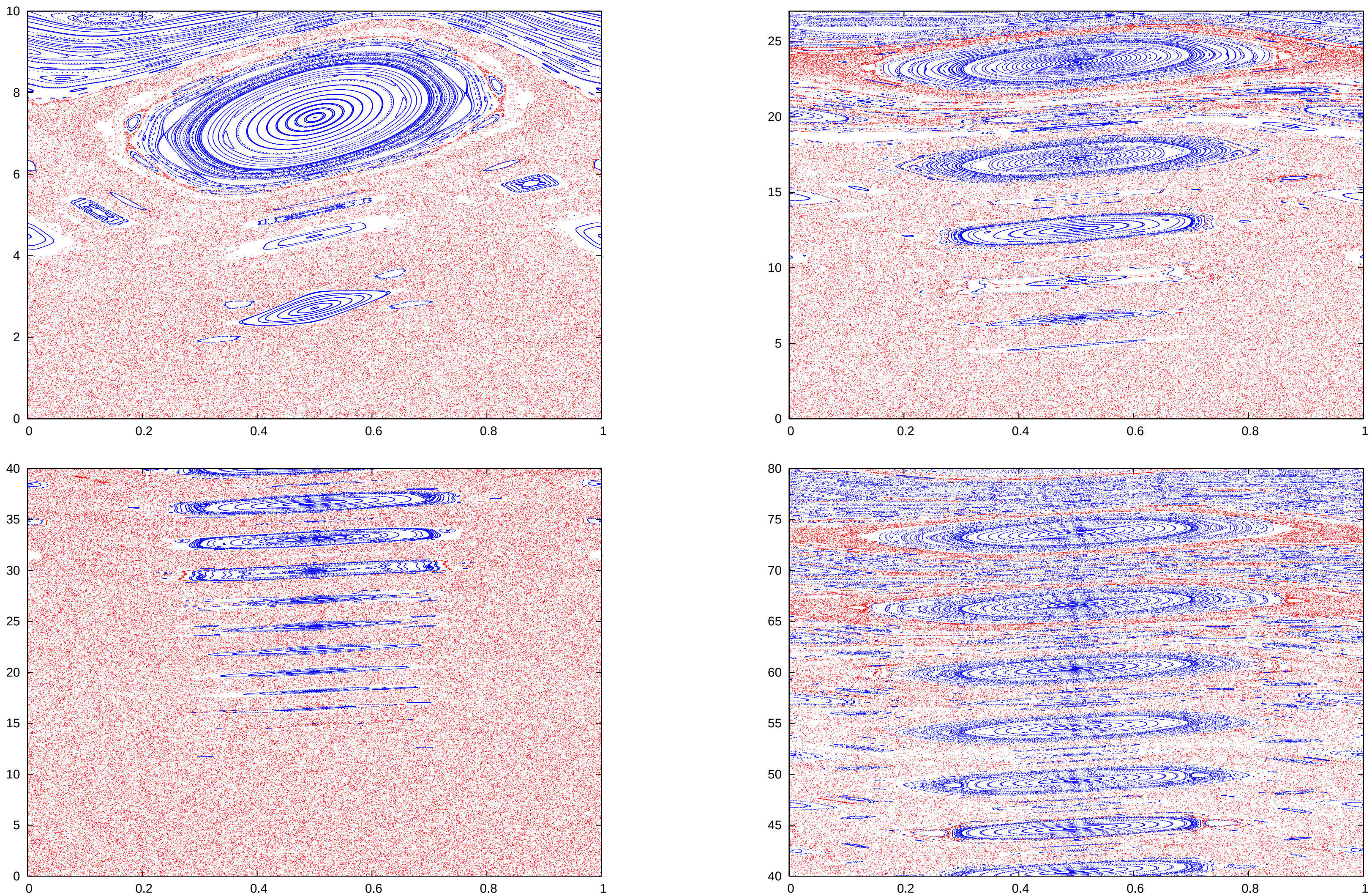

Orbits of SM: positive Lyapunov exponent in red. Top left: $b = 1$; right: $b = \sqrt{10}$. Bottom: $b = 10$. Left $y < 40$; rigth $y > 40$.

The biseparatrix map

For some cases, like the transition for $c \in [1.014, 1.015]$ there are **chains of islands**, the first and last ones very narrow and become larger in the central part. The SM is not a good model for this.

Not only one but **two separatrices** play a relevant role in the creation of these islands.

A similar thing occurs in the **Birkhoff zones**. Consider an APM around an elliptic fixed point. One can have an **annular domain** bounded by rotational invariant curves. Between these curves one can have islands but maybe not other rotational invariant curve. This is paradigmatic for APM. A suitable scheme is shown.

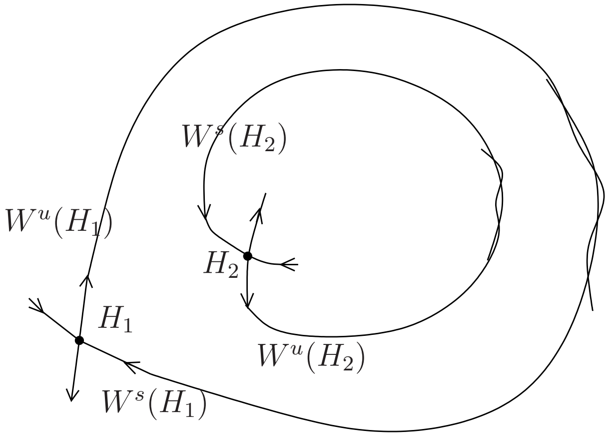

The effect of the **lower separatrix** is described by a SM. If there is an **upper separatrix** near $y = d$ one can consider the domain $0 < y < d$ and a simple model like

$$BS\begin{pmatrix} x \\ y \end{pmatrix} = \begin{pmatrix} \bar{x} \\ \bar{y} \end{pmatrix} = \begin{pmatrix} x + a + b_1 \log(\bar{y}) - b_2 \log(d - \bar{y}) \\ y + \sin(2\pi x) \end{pmatrix}.$$

where $d, b_1, b_2 > 0$ and x mod 1. The negative sign in front of b_2 is due to the change of orientation of the upper and lower invariant manifolds.

We shall denote this map as the **biseparatrix map**. Should be understood as a **qualitative paradigm** rather than **quantitative**.

As before, assuming $d >> 1$, $y_0 >> 1$, $d - y_0 >> 1$ and $y = y_0 + r, r = O(1)$, the map BS is approximated by a SM as

$$BS\begin{pmatrix} x \\ r \end{pmatrix} = \begin{pmatrix} \bar{x} \\ \bar{r} \end{pmatrix} \approx \begin{pmatrix} x + \hat{a} + \left(\frac{b_1}{y_0} + \frac{b_2}{d - y_0}\right)\bar{r} \\ r + \sin(2\pi x) \end{pmatrix}.$$

where now $\hat{a} = a + b_1 \log(y_0) - b_2 \log(d - y_0)$. Again the condition **to exist invariant curves** can be written as

$$\frac{b_1}{y_0} + \frac{b_2}{d - y_0} < \varepsilon_G.$$

The minimum, with respect to y_0, of the left side in the inequality is obtained for $y_0 = d\frac{\sqrt{b_1}}{\sqrt{b_1}+\sqrt{b_2}}$ and equals

$$(\sqrt{b_1} + \sqrt{b_2})^2/d.$$

If this is $> \varepsilon_G$ **there are no rotational invariant curves** in the annulus. Otherwise curves appear in a central strip (depending on the relative values of b_1, b_2.)

It is possible to analyze the existence of **elliptic fixed points** (and therefore **islands**) in the annulus. Assuming, for simplicity $a = 0$, we obtain $x = 0$ or $x = 1/2$ and $b_1 \log(y) - b_2 \log(d - y) = k \in \mathbb{Z}$.

Last equation is transcendental if $b_2/b_1 \notin \mathbb{Q}$, but it has solution for all k. If $k \to -\infty$ (resp. $k \to \infty$) the solution tends to $y = 0$ (resp. to $y = d$).

The simplest case is $b_1 = b_2 = b$. Asking for $|\mathrm{tr}(DBS)| < 2$ then $x = 1/2$, $y = b(1/y + 1/(d - y) < 4/(2\pi)$. Let $\gamma = \exp(k/b) > 0$. This requires $d > 2\pi b$ to have elliptic points and the corresponding k satisfy $-k_{\max} < k < k_{\max}$, where $k_{\max} = E[b\xi]$ with $\xi = \cosh^{-1}\left(\frac{d}{\pi b} - 1\right)$.

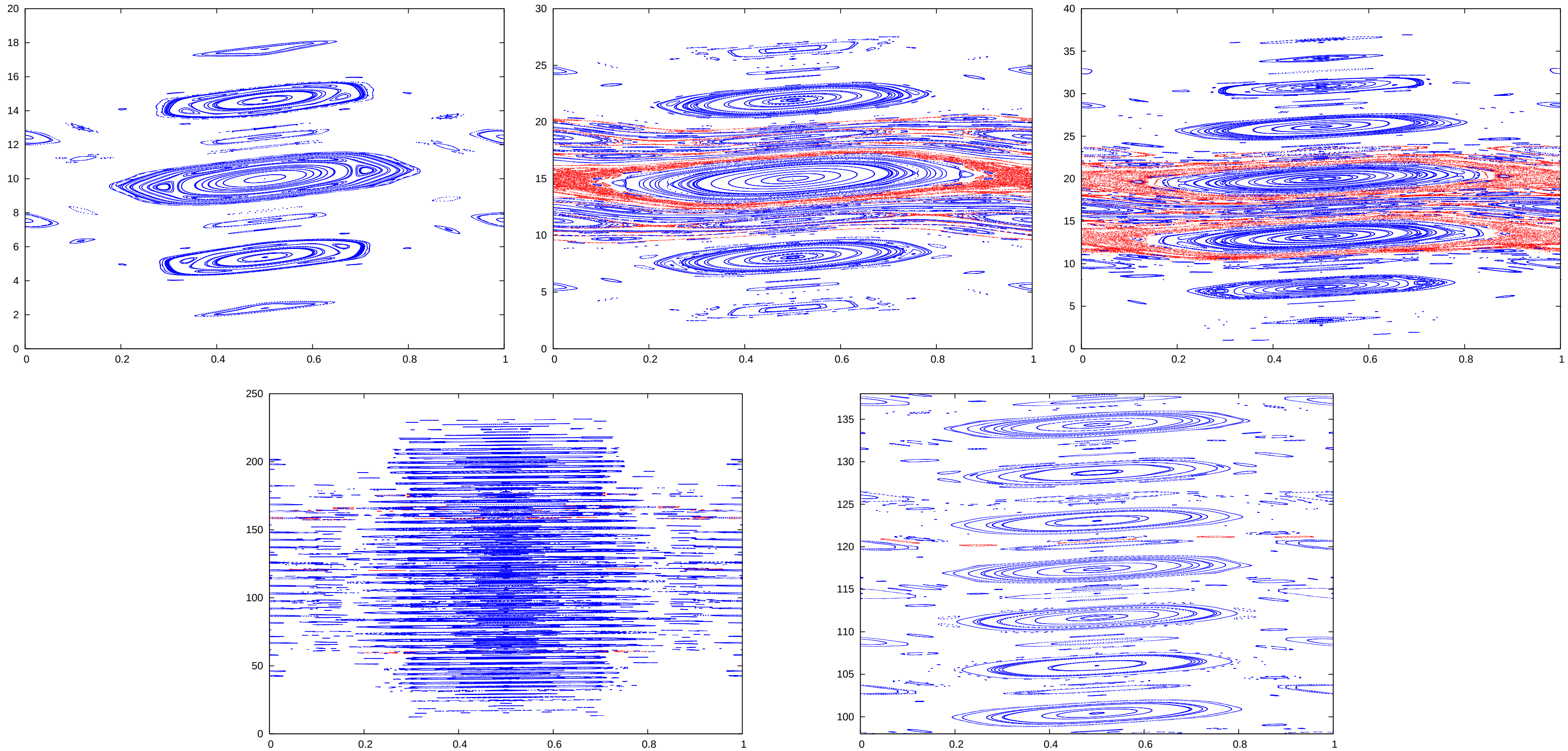

Dynamics of the biseparatrix map. Top left $(b_1, b_2, d) = (1, 1, 20)$; center $(b_1, b_2, d) = (1, 1, 30)$; right $(b_1, b_2, d) = (1, 3, 40)$. Bottom left $(b_1, b_2, d) = (10, 12, 250)$ and a detail to the right.

Points with an iterate satisfying $y \notin (0, d)$ have been discarded. Otherwise 10^7 iterates have been used to compute the Lyapunov exponent Λ. Last 1000 iterates are plotted in blue if $\Lambda < 2 \times 10^{-6}$. Else, in red.

Other relevant features of the Hénon map

Rotation number

We use a **different representation**

$$H_\alpha : \begin{pmatrix} x \\ y \end{pmatrix} \longmapsto R_{2\pi\alpha} \begin{pmatrix} x \\ y - x^2 \end{pmatrix},$$

also equivalent to

$$H_a : \begin{pmatrix} u \\ v \end{pmatrix} \to \begin{pmatrix} 1 - au^2 + v \\ -u \end{pmatrix}$$

via $a = \cos^2(2\pi\alpha) - 2\cos(2\pi\alpha)$ and $c = \sqrt{(1+a)}$ and suitable changes of coordinates. H_α has elliptic point E at the origin and hyperbolic at $(2\tan(\pi\alpha), 2\tan^2(\pi\alpha)$. It is **reversible** with respect to $y = \tan(\pi\alpha)x$ and with respect to parabola $y = x^2/2$ by means of the involutions $(x, y) \mapsto (\cos(2\pi\alpha)x + \sin(2\pi\alpha)y, \sin(2\pi\alpha)x - \cos(2\pi\alpha)y)$ and $(x, y) \mapsto (x, x^2 - y)$, respectively.

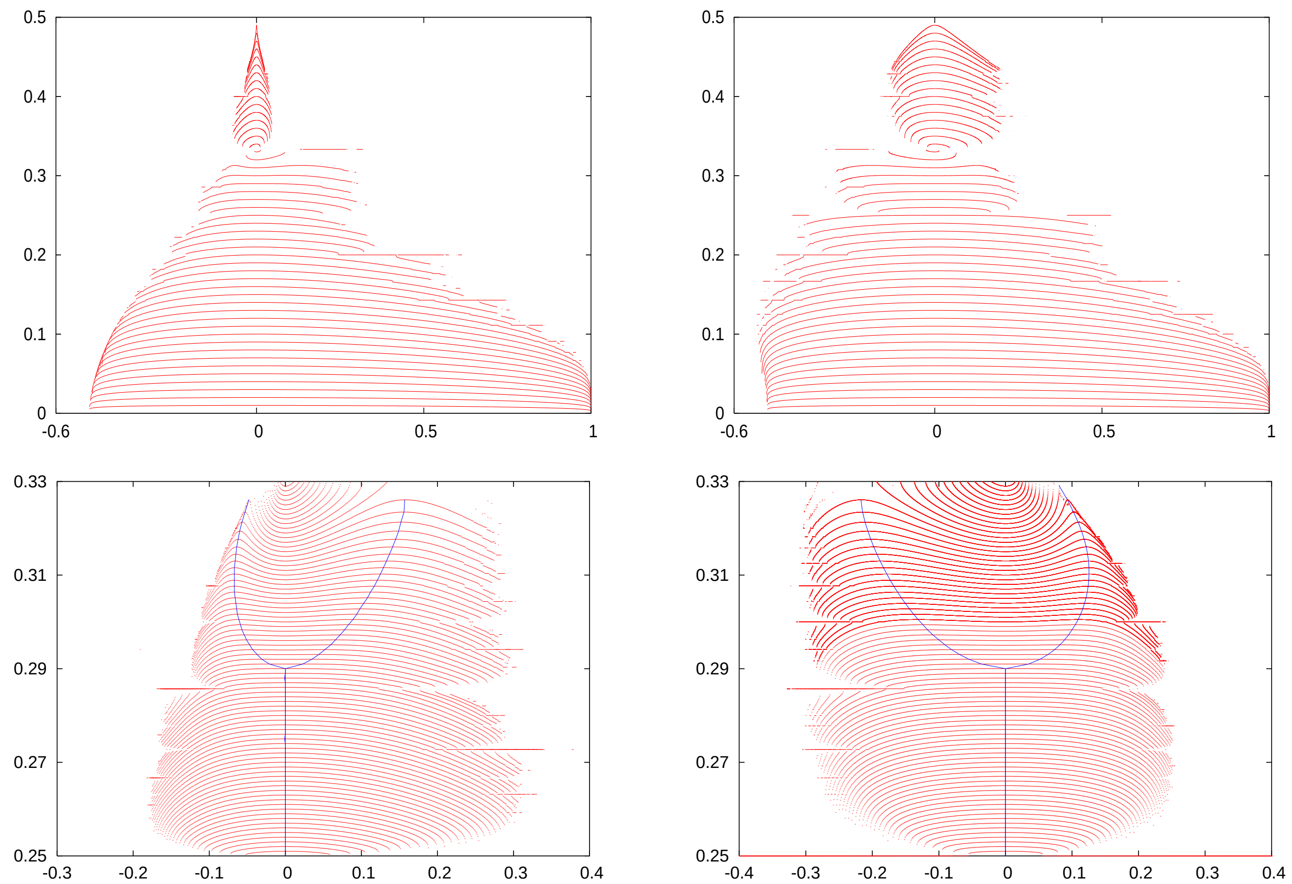

Representation of the rotation number ρ (y-axis) as a function of the (normalised) distance to the origin (x-axis). Bottom: Magnification of the above figures. The blue line joins **local maxima** of the rotation number for each α. Left pictures are obtained taking initial points on $y = \tan(\pi\alpha)x$ while right ones on the curve $y = x^2/2$.

Looking to the details one can "see" the location of different **resonances**.

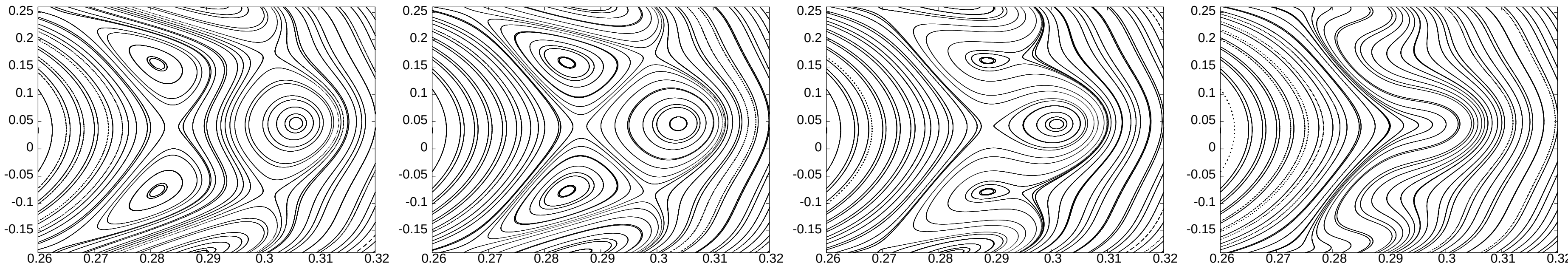

The existence of local maxima implies **failure of the twist condition**. This gives rise, generically, to **meandering curves**. They are invariant, rotational, but **not graphs** if we try to express radius with respect to E as a function of the angle. The used values of α, from left to right, are 0.299546 to 0.299543 with step -10^{-6}. The islands have rotation number $3/10$.

The existence of local maxima is related to the **change of sign** of the **first Birkhoff coefficient of the Normal Form** which occurs for the zero of $-2\sin(4\hat{\alpha}) + \sin(3\hat{\alpha}) + \sin(2\hat{\alpha}) + 3\sin(\hat{\alpha})$, where $\hat{\alpha} = 2\pi\alpha$ ($\alpha \approx 0.2902153116276$).

Normal Forms: the Resonant Case

It is convenient to use a **complex representation** $z = x + \mathrm{i}\, y$ and then H_α reads

$$z \longmapsto \lambda z - \frac{\lambda}{4}\mathrm{i}\, z^2 - \frac{\lambda}{2}\mathrm{i}\, z\bar{z} - \frac{\lambda}{4}\mathrm{i}\, \bar{z}^2,$$

where $\lambda = \exp(2\pi\mathrm{i}\,\alpha)$.

To obtain the **Normal Form** of an APM F we do (**symplectic**) changes to cancel as many terms as possible. All terms of the form $z^j \bar{z}^k$ with $j, k \in \mathbb{N}$ can be cancelled if the **non-resonance condition** $\lambda^{j-k-1} \neq 1$, $j + k \geq 2$ holds. Terms with $j = k + 1$ should be kept (the **unavoidable resonances**).

To study the vicinity of a resonance we want a NF valid **around the resonance**. If $\alpha = \frac{q}{m} + \delta$, $1 < q < m$, $(q, m) = 1$ and δ small we shall have, for $j = 0, k = m - 1$, that $\lambda^{j-k-1} \simeq 1$. This term must be kept. Up to order m we have (keeping the name F for the map)

$$F : z \longmapsto \lambda z + a_1 z^2 \bar{z} + \cdots + a_s z^{s+1} \bar{z}^s + + \tilde{c}\bar{z}^{m-1} + \tilde{\mathcal{R}}_m(z, \bar{z}),$$

where $a_i \in \mathbb{C}$, $s = [m/2] - 1$ and $\tilde{\mathcal{R}}_m = O(|z|^m)$.

Introducing **Birkhoff coefficients,** $b_i \in \mathbb{R}$ we have

$$z \longmapsto R_{2\pi\frac{q}{m}}\left(e^{2\pi i\gamma(r)}z + c\bar{z}^{m-1}\right) + \mathcal{R}_m(z,\bar{z}),$$

where $R_{2\pi\frac{q}{m}}$ denotes the rigid rotation of angle $2\pi q/m$ and

$$\gamma(r) = \delta + b_1 r^2 + b_2 r^4 + \cdots + b_s r^{2s},\ r^2 = |z|^2.$$

Skipping the remainder we have the **Normal Form to order** $m-1$

$$NF_m(F) : z \longmapsto R_{2\pi\frac{q}{m}} \circ K(z,\bar{z},\delta),$$

where $K(z,\bar{z},\delta) = e^{2\pi i\gamma(r)}z + c\bar{z}^{m-1}$. Remark that the two maps in $NF_m(F)$ commute. Then $NF_m(F)^m = K^m$. Enough to study K.

Approximation by a flow: K can ve approximated by the flow with Hamiltonian

$$\mathcal{H}(I,\varphi) = \mathcal{H}_{nr}(I) + \mathcal{H}_r(I,\varphi),$$

$\mathcal{H}_{nr}(I) = \pi\sum_{n\geq 0}\frac{b_n}{n+1}(2I)^{n+1}$, $(b_0 = \delta)$, $\mathcal{H}_r(I,\varphi) = \frac{1}{m}(2I)^{\frac{m}{2}}\cos(m\varphi)$.

The Poincaré variables (I, φ) are defined by

$$(I, \varphi) = \left(\frac{|z|^2}{2}, \arctan\left(\frac{z - \bar{z}}{i(z + \bar{z})} \right) \right).$$

Then $\hat{K}(I, \varphi) = \phi_{t=1}(I, \varphi) + O\left(I^{\frac{m+1}{2}}\right)$.

The resonant zone of order $m > 4$: In first aproximation given by $\gamma(r^*) = 0$, i.e., $I^* = -\delta/(2b_1)$ assuming, e.g. $b_1 > 0$.

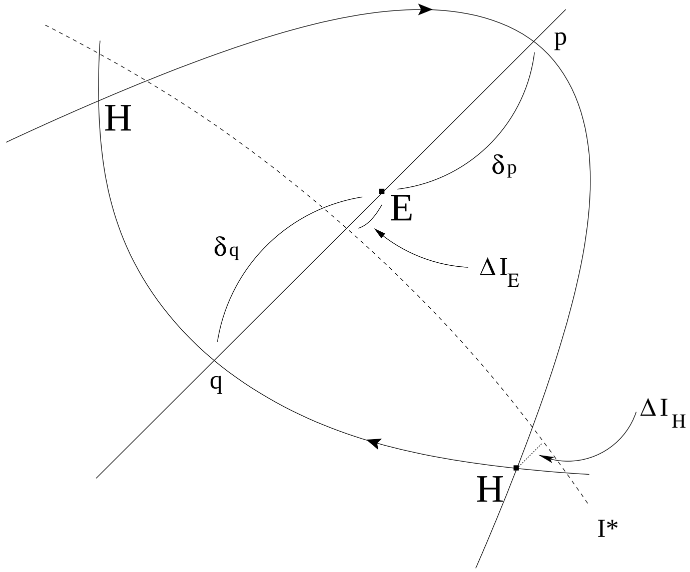

$\delta_p = \sqrt{\frac{(2I_*)^{m/2}}{m\pi b_1}}(1+O(I_*^{\mu}))$, δ_q similar, $\Delta I_E = \frac{(2I^*)^{m/2-1}}{4\pi b_1}(1+O(I_*))$, ΔI_H similar.

The dynamics around a resonant island: Described by Hamiltonian

$$\mathcal{H}(J,\psi) = \frac{1}{2}J^2 + \frac{c}{3}J^3 - (1 + dJ)\cos(\psi),$$

where $c = O(|b_2|\,|b_1|^{(6+m)/4}|\delta|^{m/4})$, $d = O(|b_1|^{(2+m)/4}|\delta|^{m/4-1})$, $J = I - I^*$, $\psi = m\varphi$.

Remarks: c and b_2 have the same sign, $d > 0$, $|c| < d$.

Going back to F note the existence of **inner and outer splittings**. Close to the central elliptic point the behaviour is related to the **first two Birkhoff coefficients**. Far away is related to the **first and second derivatives of ρ**, the rotation number of an integrable approximation.

Let F be an APM with resonance strip located near $I = I^*$ verifying

$$\frac{d\rho}{dI}|_{I=I^*} \neq 0, \; \frac{d^2\rho}{dI^2}|_{I=I_*} \neq 0.$$

Then, the islands of the resonance have, generically, **both splittings different**. Ignoring higher order terms, **outer splitting $>$ inner one** provided one of these hold

(a) $\left.\frac{d\rho}{dI}\right|_{I=I^*} > 0$ and $\left.\frac{d^2\rho}{dI^2}\right|_{I=I^*} > 0$ or $\left.\frac{d^2\rho}{dI^2}\right|_{I=I^*} \lessapprox 0$,

(b) $\left.\frac{d\rho}{dI}\right|_{I=I^*} < 0$ and $\left.\frac{d^2\rho}{dI^2}\right|_{I=I^*} < 0$ or $\left.\frac{d^2\rho}{dI^2}\right|_{I=I^*} \gtrapprox 0$.

Otherwise, **the inner is greater than the outer**.

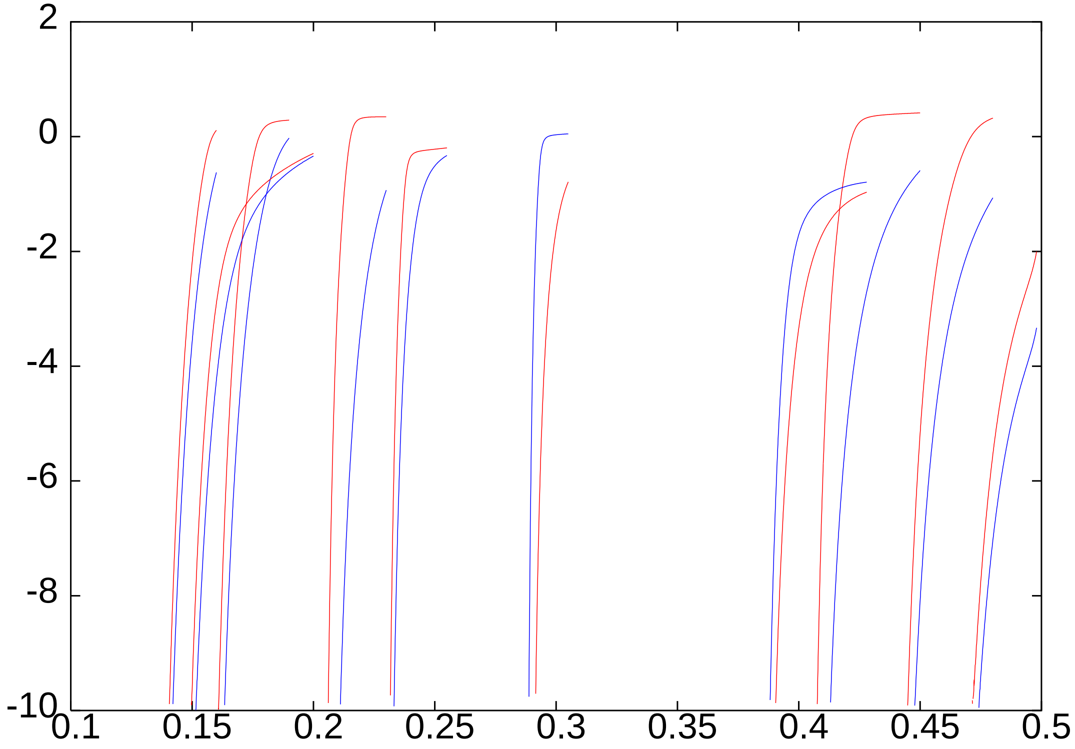

$\log_{10}$ of splittings vs α. Red for outer, blue for inner. Resonances (1:9), (1:8), (1:7), (1:5), (2:9), (2:7), (3:8), (2:5), (3:7) and (4:9).

Rates of escape

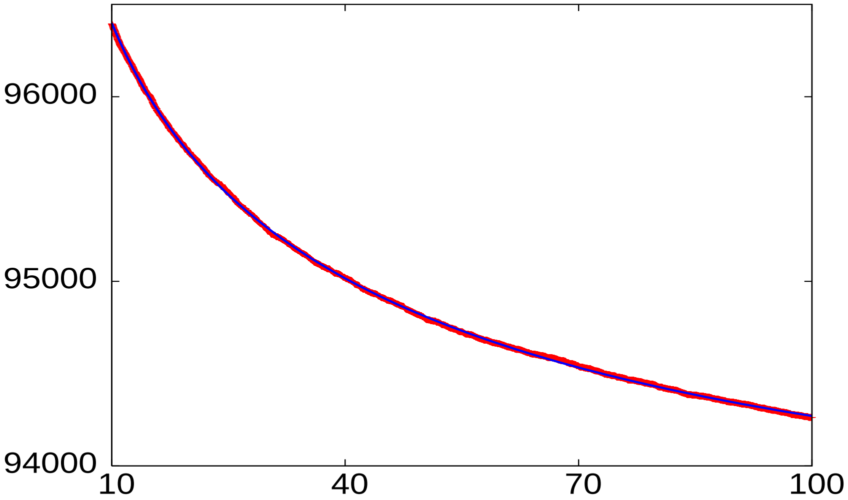

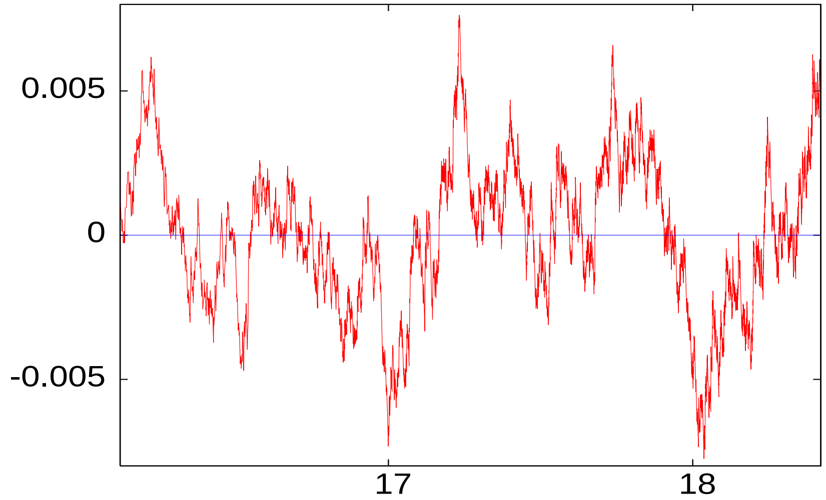

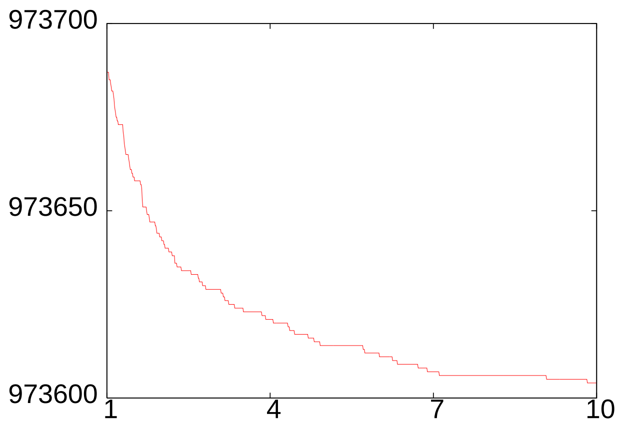

Top: For the previous figure $c = 1.017$, subsisting points $s(N)$ vs N (in millions) and graph of fit $a + b\exp(-cN^d)$, where $d \approx 0.4$, and plot of $\log(-\log((s(N) - a)/b)) - \log(cN^d)$ vs $\log(N)$. Bottom: $s(N)$ vs N for the figure with $c = 0.4$, for comparison.

The case $c = 1.5$

Local instability from **NF**. What about **globally**?

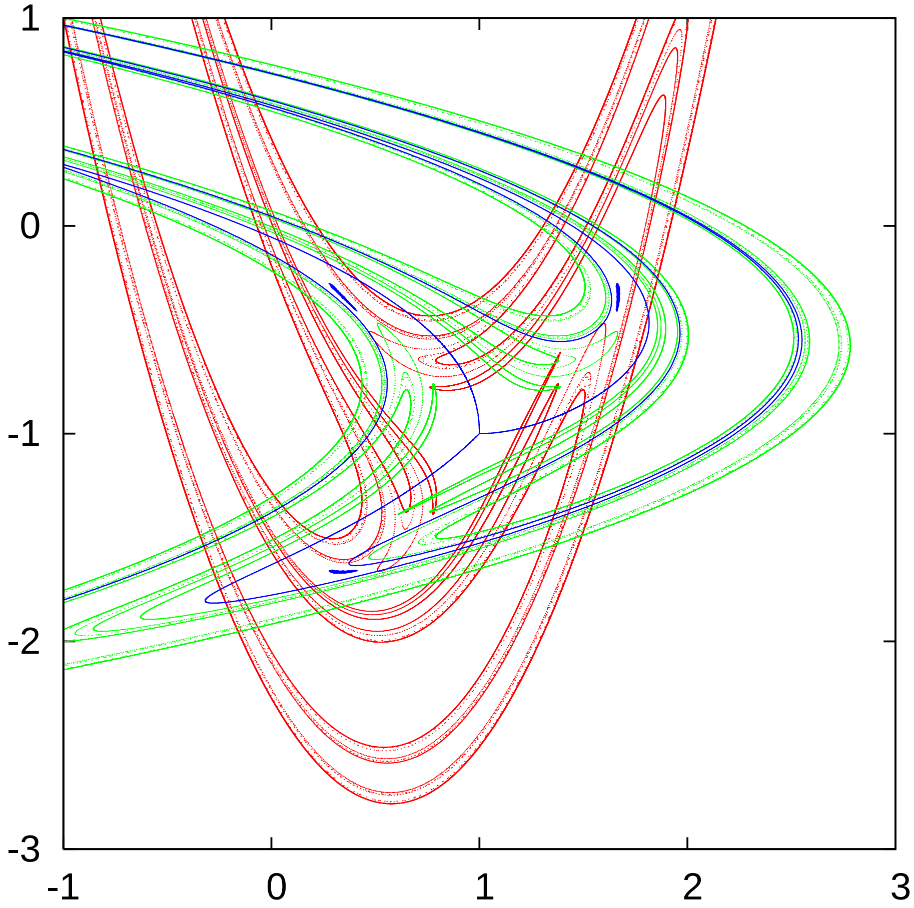

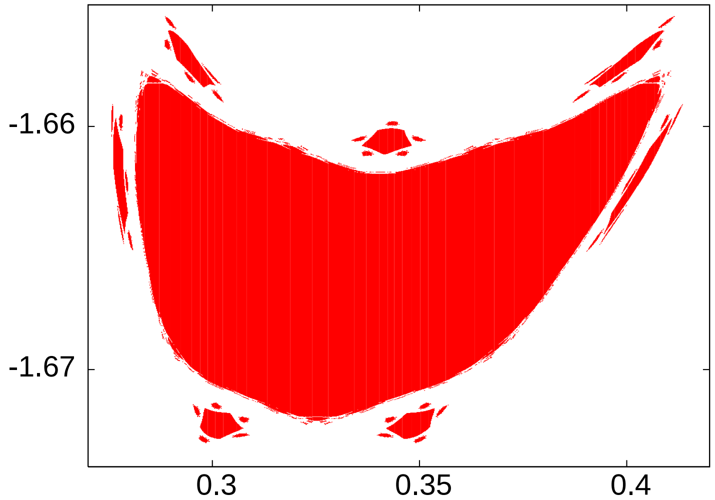

W^s, W^u of hyperbolic point H in red and green, resp. Branches of W^u of "elliptic" point E in blue. Also in blue a **period 3 island** magnified to the right.

Regularity of invariant manifolds

In all previous cases W^s, W^u of H are **analytic** (in fact **entire**). A **parametric representation** is used. But for E the branches are only **Gevrey**. Computed as a **graph**: $y+1=\sum_{k\geq 2} a_k(x-1)^k$.

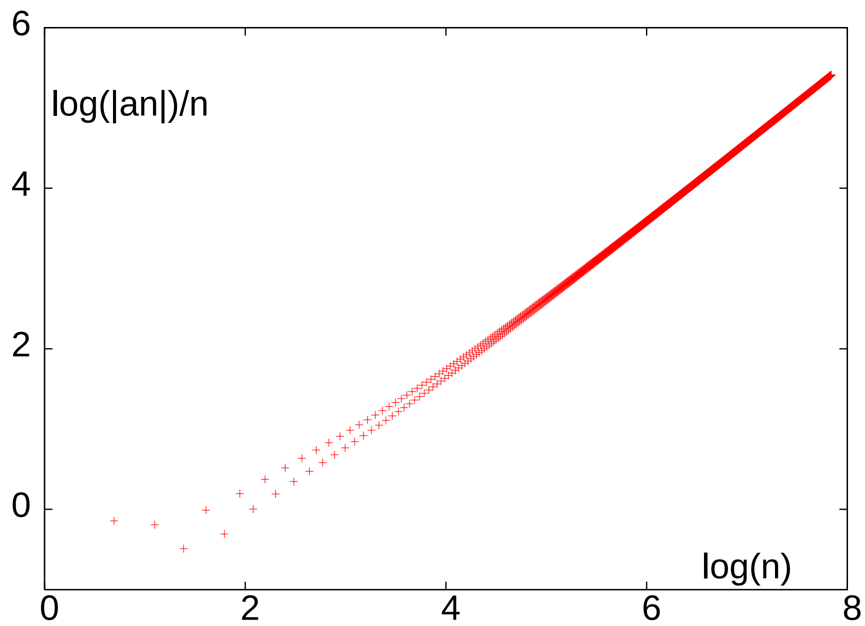

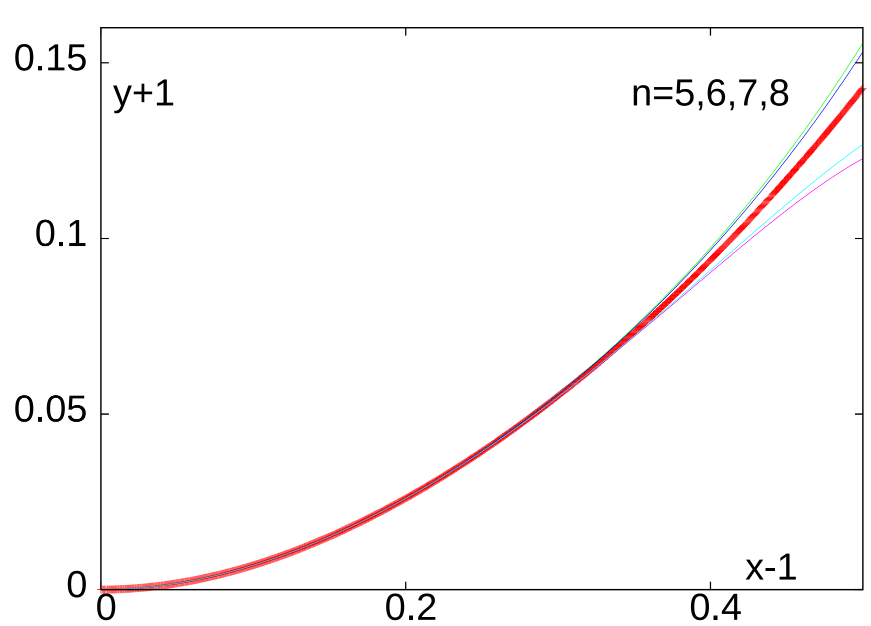

Left: Values of $\log(|a_n|^{1/n})$ vs $\log(n)$. A fit gives **slope** very close to **1**. Right: Local plot of the manifold and **approximations** of degrees $5, 6, 7, 8$.

$a_n > 0$ (resp. $a_n < 0$) if n is congruent with $0, 1$ (resp. $2, 3$) modulus 4.

What about theoretical proofs of the observed numerical evidences?

Of course, these numerical experiments prove nothing in the mathematical sense, but give good hints about the location of curves close to the last invariant curve.
To convert these results into a proof one needs

- Concerning the invariant curve: To produce a Fourier approximation of the invariant curve, to obtain a normal form around it with rigorous estimate of the remainder and to apply KAM theory.
- Concerning the existence of nearby points which escape: To find a heteroclinic chain of transversal intersections with initial manifold close to the invariant curve and with final manifold the one of the H point.

Both computations have to be done using interval arithmetic (or any other method giving rigorous estimates) and require a finite (may be long) number of computations (may be multiple precision).
This kind of **CAP** (Computer Assisted Proof) is feasible in both cases with the methods known at present.

Taylor integration method

Consider an IVP for an ODE like

$$\dot{x} = f(t,x), \qquad x(t_0) = x_0,$$

where f is assumed to be analytic in a nbd of $(t_0, x_0) \in \Omega \subset \mathbb{R} \times \mathbb{R}^n$.

We want to produce **in an easy way** the **Taylor expansion** $x(t_0 + h)$ for suitable values of h and use it as a one-step method.

For a very large class of functions the evaluation of f can be split in simple expressions

$$\begin{aligned}
e_1 &= g_1(t,x), \\
e_2 &= g_2(t,x,e_1), \\
&\vdots \\
e_j &= g_j(t,x,e_1,\ldots,e_{j-1}), \\
&\vdots \\
e_m &= g_m(t,x,e_1,\ldots,e_{m-1}), \\
f_1(t,x) &= e_{k_1}, \\
&\vdots \\
f_n(t,x) &= e_{k_n},
\end{aligned}$$

where each one of the expressions e_j contains a sum of arguments, a product or quotient of two arguments or an elementary function (like sin, cos, log, exp, $\sqrt{\,}, \ldots$) of a single argument.
The basic idea is to compute in a **recurrent way** the **power series expansion** of all the e_j. All the g_j have to be seen as **operations with (truncated) power series**. The input are t and the coefficients of order 0 of the components of x_0. At the end of first step we know the terms of order 1 of these components. If the terms up to order s of the arguments of the g_j are known, we obtain easily the coefficient of order s of e_j.
Hence the representation of the components x_i of $x(t_0 + h)$ looks like

$$x_i = \sum_{s=0}^{N} a_i^{(s)} h^s.$$

There are several **strategies** to select **order and step** to have, approximately, some **desired truncation error**. Also to save computing time (like multiplying by a precomputed $1/s$ instead of dividing by s), but some **caution** is required to avoid systematic errors.

Some **elementary recurrences**

Let $a(t) = \sum_{k\geq 0} a_k t^k, \quad b(t) = \sum_{k\geq 0} b_k t^k$, etc.

$c = a * b: \quad c_n = \sum_{k=0}^{n} a_k b_{n-k}$

$c = a/b,\ b_0 \neq 0, \quad c_0 = a_0/b_0, \quad c_n = \frac{1}{b_0}\left[a_n - \sum_{k=0}^{n-1} c_k b_{n-k}\right],\ n > 0$

$c = a^\alpha,\ \alpha \in \mathbb{R},\ a_0 \neq 0, \quad c_0 = a_0^\alpha,$
$\quad c_n = -\frac{1}{n a_0} \sum_{k=0}^{n-1} c_k a_{n-k}[k - \alpha(n-k)],\ n > 0$

$c = \exp(a), \quad c_0 = \exp(a_0), \quad c_n = \frac{1}{n} \sum_{k=0}^{n-1} c_k a_{n-k}(n-k),\ n > 0$

$c = \log(a),\ a_0 \neq 0, \quad c_0 = \log(a_0), \quad c_n = \frac{1}{n a_0}\left[n a_n - \sum_{k=1}^{n-1} k c_k a_{n-k}\right],$
$\quad n > 0$

$c = \cos(a),\ s = \sin(a), \quad c_0 = \cos(a_0),\ s_0 = \sin(a_0),$
$\quad c_n = -\frac{1}{n} \sum_{k=0}^{n-1} s_k a_{n-k}(n-k), \quad s_n = \frac{1}{n} \sum_{k=0}^{n-1} c_k a_{n-k}(n-k),\ n > 0$

For **many other functions** (e.g. Bessel functions) one can **add** to the list of ODE **the differential equations that these functions satisfy**.

Some interesting properties

- Under reasonable conditions the **optimal stepsize** (concerning efficiency for fixed truncation error) is almost independent of the number of digits.
- The **optimal order** is approximately linear in the number of digits.
- The **computational cost** (measured in number of elementary operations) is approximately quadratic in the number of digits.

Some elementary **pitfalls** are shown in the next figures, for the integration of $\dot{x} = -y$, $\dot{y} = x$. The order used is $N = 24$, the local tolerance is 10^{-21} and the final time $2\pi \times 10^9$. Different runs use **multiplication** by $1/s$ instead of **division** by s to obtain $a_i^{(s)}$ from some s_0 on. The plots show **absolute errors** in energy as a function of t and the **average slope of the energy** as a function of t, both for several values of s_0.

It is also convenient to use **truncation errors** **small** compared to the ε **of the processor**, to avoid biases, so that these errors **can be neglected**. Only **roundoff errors** and its **propagation by the dynamics** turns out to be **relevant**.

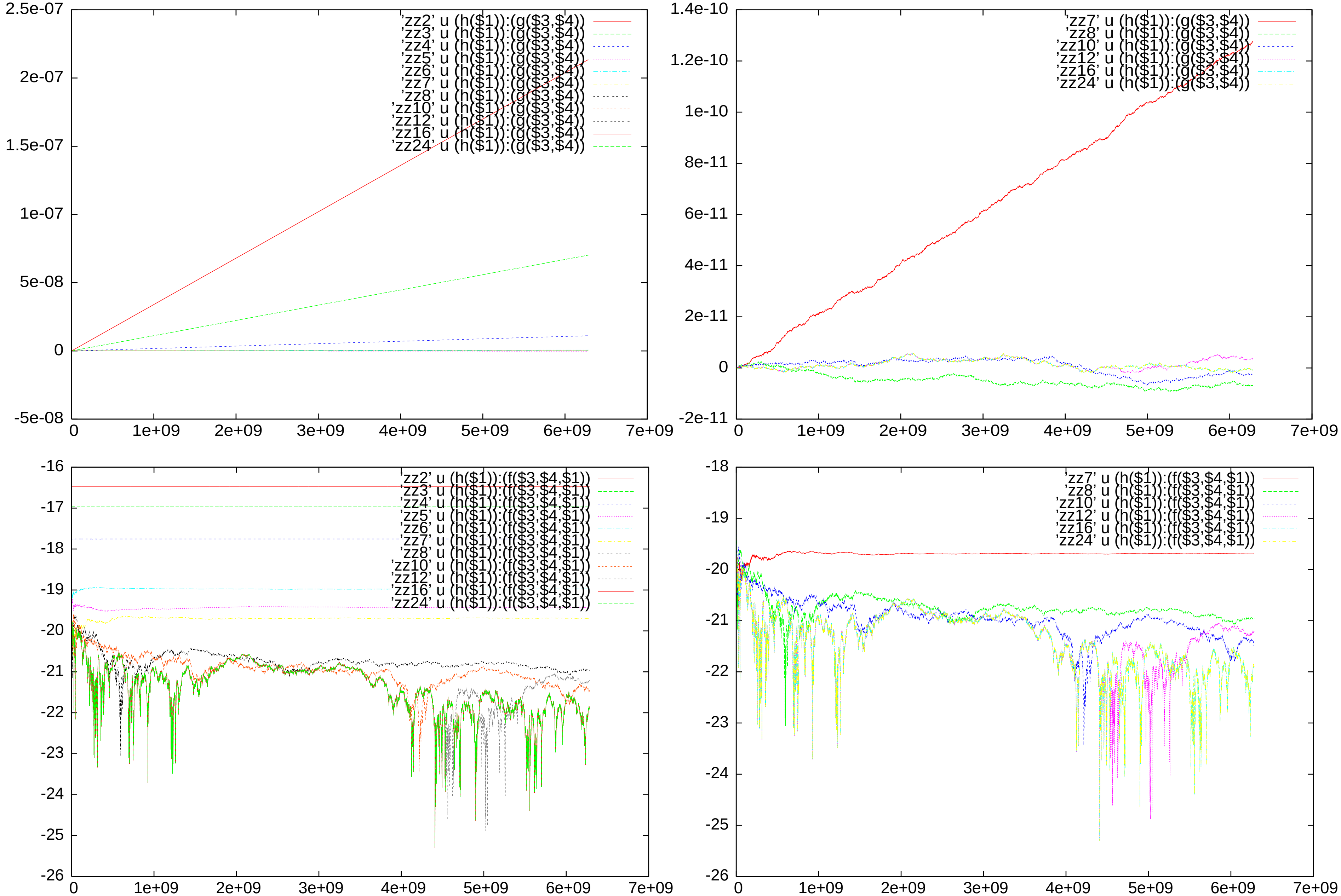

'zz2' u (h($1)):(g($3,$4))
'zz3' u (h($1)):(g($3,$4))
'zz4' u (h($1)):(g($3,$4))
'zz5' u (h($1)):(g($3,$4))
'zz6' u (h($1)):(g($3,$4))
'zz7' u (h($1)):(g($3,$4))
'zz8' u (h($1)):(g($3,$4))
'zz10' u (h($1)):(g($3,$4))
'zz12' u (h($1)):(g($3,$4))
'zz16' u (h($1)):(g($3,$4))
'zz24' u (h($1)):(g($3,$4))
2.5e-07
2e-07
1.5e-07
1e-07
5e-08
0
-5e-08
'zz7' u (h($1)):(g($3,$4))
'zz8' u (h($1)):(g($3,$4))
'zz10' u (h($1)):(g($3,$4))
'zz12' u (h($1)):(g($3,$4))
'zz16' u (h($1)):(g($3,$4))
'zz24' u (h($1)):(g($3,$4))
1.4e-10
1.2e-10
1e-10
8e-11
6e-11
4e-11
2e-11
0
-2e-11
'zz2' u (h($1)):(f($3,$4,$1))
'zz3' u (h($1)):(f($3,$4,$1))
'zz4' u (h($1)):(f($3,$4,$1))
'zz5' u (h($1)):(f($3,$4,$1))
'zz6' u (h($1)):(f($3,$4,$1))
'zz7' u (h($1)):(f($3,$4,$1))
'zz8' u (h($1)):(f($3,$4,$1))
'zz10' u (h($1)):(f($3,$4,$1))
'zz12' u (h($1)):(f($3,$4,$1))
'zz16' u (h($1)):(f($3,$4,$1))
'zz24' u (h($1)):(f($3,$4,$1))
-16
-17
-18
-19
-20
-21
-22
-23
-24
-25
-26
'zz7' u (h($1)):(f($3,$4,$1))
'zz8' u (h($1)):(f($3,$4,$1))
'zz10' u (h($1)):(f($3,$4,$1))
'zz12' u (h($1)):(f($3,$4,$1))
'zz16' u (h($1)):(f($3,$4,$1))
'zz24' u (h($1)):(f($3,$4,$1))
-18
-19
-20
-21
-22
-23
-24
-25
-26
0
1e+09
2e+09
3e+09
4e+09
5e+09
6e+09
7e+09

A first example:
Stability of the planar circular RTBP for outer motion

Next we consider a problem similar to the Hénon map, but requiring numerical integration: The planar **circular RTBP** which describes the motion of a massless particle (think about an **asteroid**) under the gravitational attraction of two primaries (think about **Sun** and **Jupiter**) moving in circular orbit about their center of masses. The **mass ratio** of the system is $\mu = m_J/(m_S + m_J)$.

The system has a **first integral** known as **Jacobi integral** C. For large enough values of C the level of this function has 3 **connected components**: Two close to the primaries and the third one away from them. Motion in this **outer region** corresponds to bodies with perihelion at a distance larger than the Sun-Jupiter distance.

Neglecting Jupiter the motion of the massless body will be a two-body motion around the Sun. If we fix e=**eccentricity** (the so-called **osculating eccentricity**) then C determines the value of the semiaxis a.

Theorem (**V. Kaloshin et al, 2006**, in preparation)
Given μ and $C > C_0$ there exist $e_0(\mu, C)$ such that if $e > e_0$ there are bodies with initial osculating eccentricity e which escape to infinity.

For $\mu = 10^{-3}$, $C = 3.6$ the estimated value of e_0 is 0.75. Proof and application are based on Aubry-Mather theory.

Next figures show orbits of different initial points on the **Poincaré section corresponding to pericenter passages**.

Top left: e as a function of $q = a(1-e)$ for $\mu = 0$. Top right: images of several initial conditions. For $q < 1.742$ (and, probably, $q < 1.748$) there are points in a chaotic zone which can escape. For $q > 1.750$ points seems definitely that do not escape because of the existence of invariant curves. Bottom figures show magnifications. In blue a set of **invariant curves**. In the next page the curves are shown alone. For one located at the bottom (with initial $q = 1.74946$, leaving orthogonally from x axis), the iterates following on a **narrow window** and **how they occur** as a function of the number of iterates in the window are shown. **Final time** 11.25×10^7 **Jupiter revolutions**.

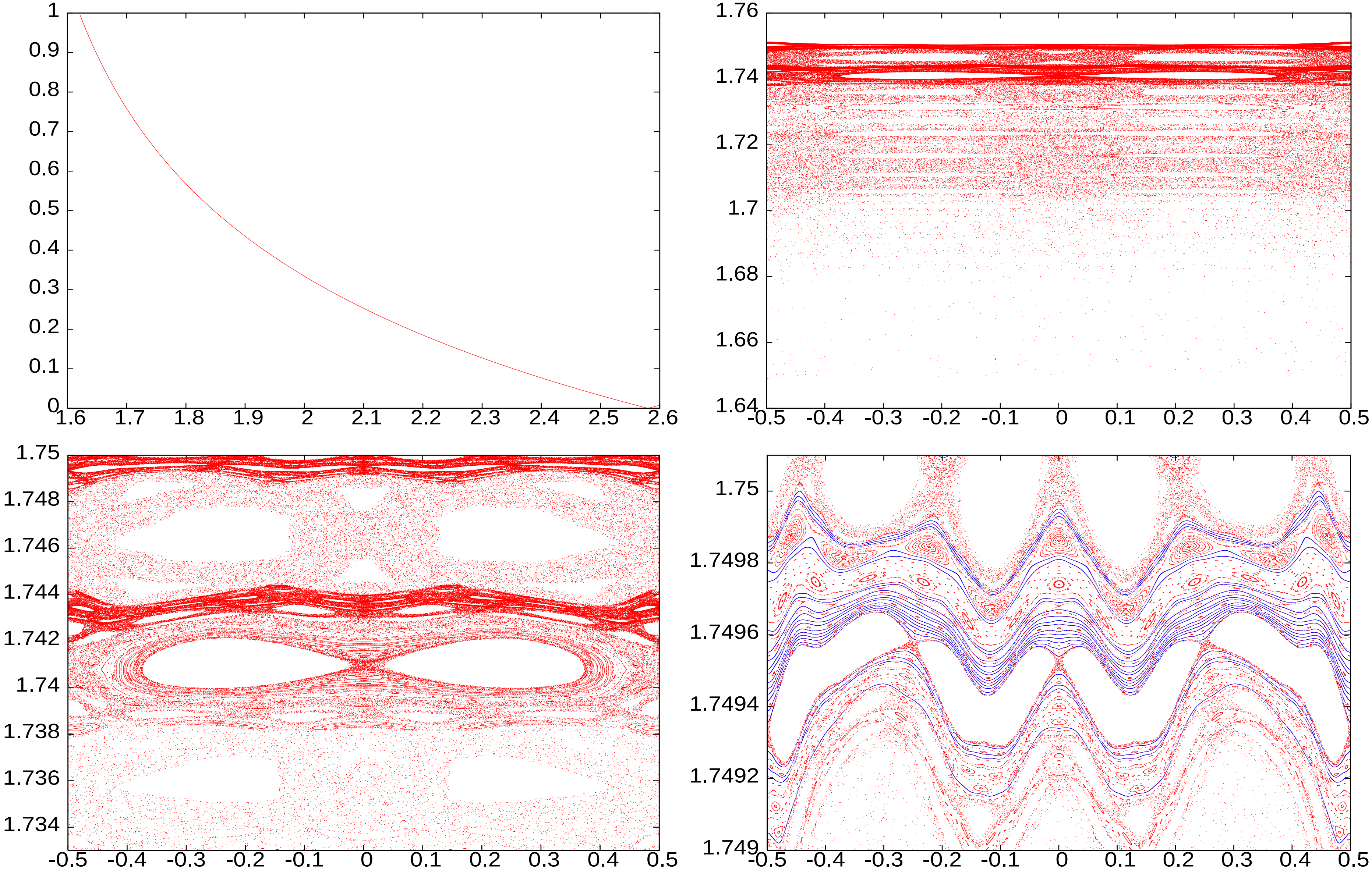

1
0.9
0.8
0.7
0.6
0.5
0.4
0.3
0.2
0.1
0
1.6
1.7
1.8
1.9
2
2.1
2.2
2.3
2.4
2.5
2.6
1.76
1.74
1.72
1.7
1.68
1.66
1.64
-0.5
-0.4
-0.3
-0.2
-0.1
0
0.1
0.2
0.3
0.4
0.5
1.75
1.748
1.746
1.744
1.742
1.74
1.738
1.736
1.734
1.75
1.7498
1.7496
1.7494
1.7492
1.749

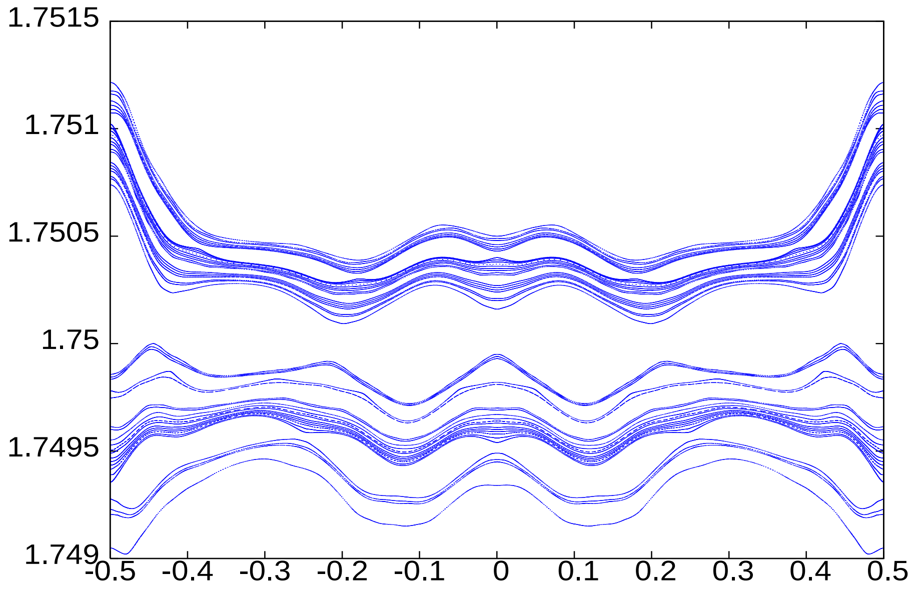

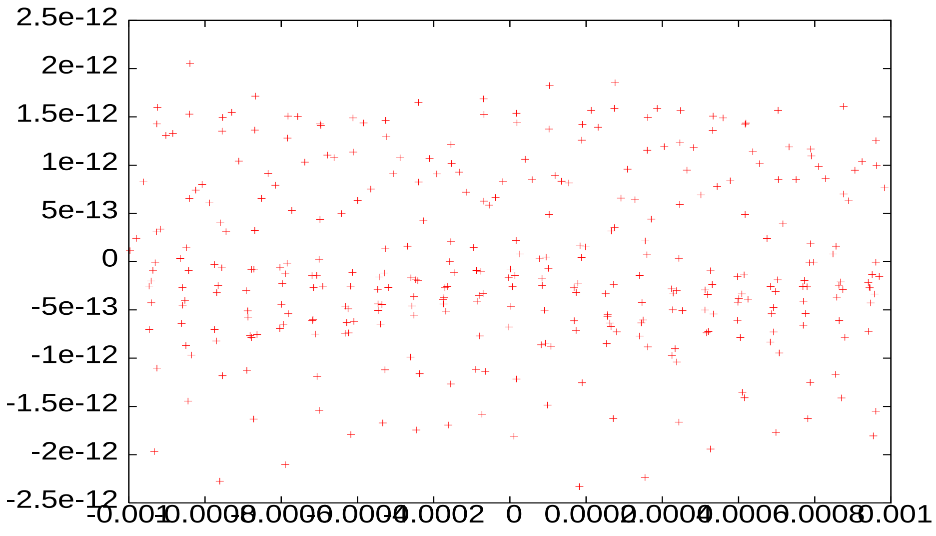

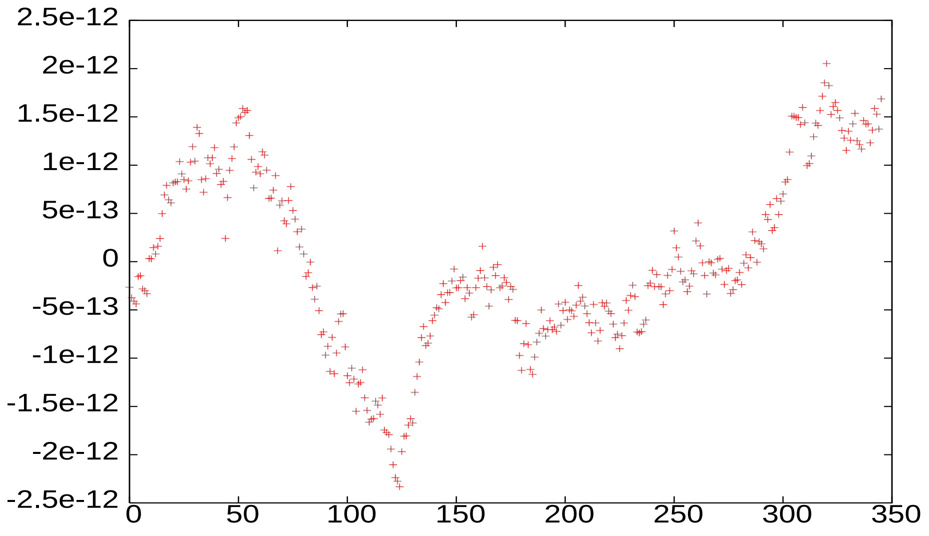

These results seem to support $0.652 < e_0 < 0.666$ for the chosen μ, C.

The effect of roundoff errors

Assuming **iid random roundoff errors** at each step the behaviour has strong relation with **the effects** of a **random walk**a.

In the **conserved quantities** the **standard deviation** σ should increase as $\sqrt{N}$ (N =number of steps) and, hence, $\approx \sqrt{t}$.

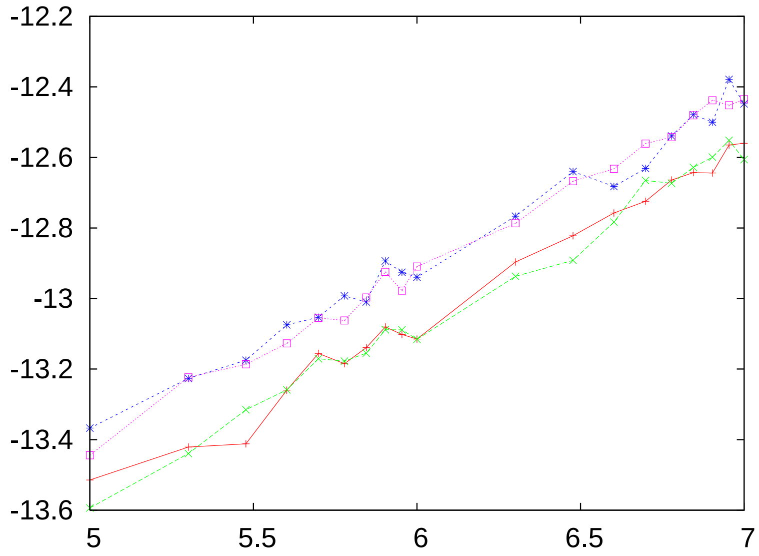

The plot shows the case of the **harmonic oscillator** (i.c. (1,0)). In $\log_{10}$ scales the horizontal axis shows **number of revolutions** and the vertical one σ (for a sample of 100 runs with minor random initial variations) of (x, y) at **the end** and the same when **returning back** to $t = 0$.

Slope $\approx 1/2$.

But the h.o. is **isochronous**. If **angular velocities change when actions do** then under same assumptions σ must change like $\approx t^{3/2}$ for integrable systems.

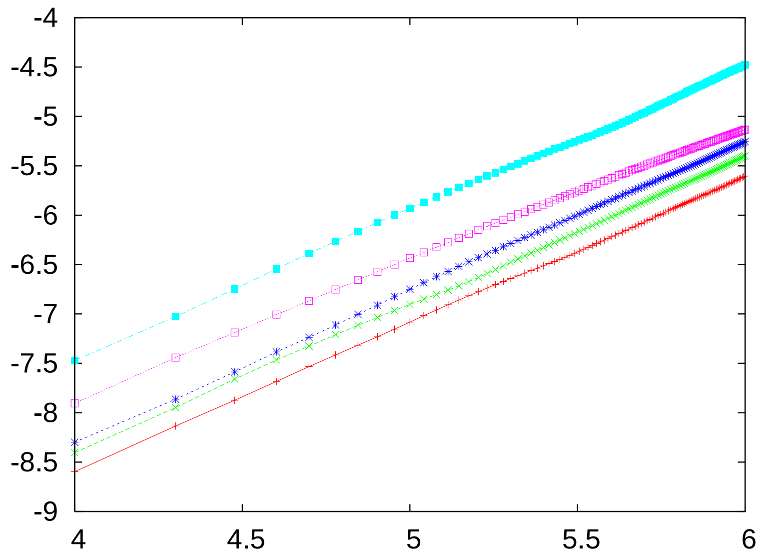

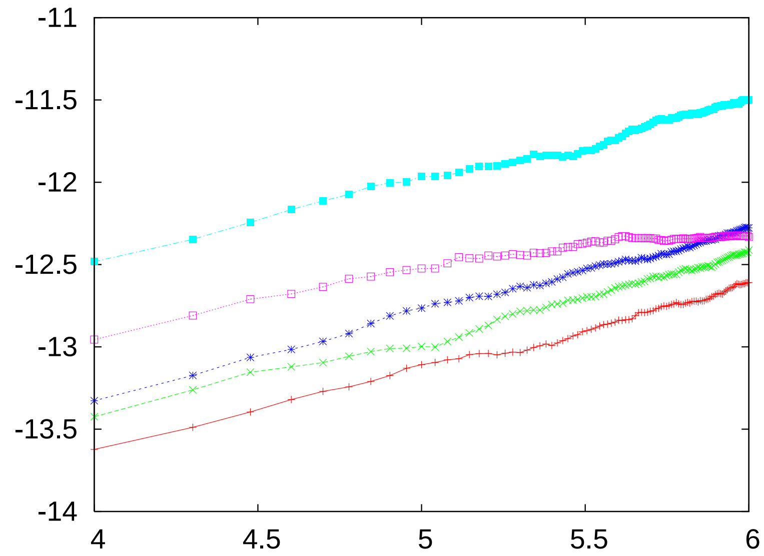

Kepler's problem for $a = 1$, $T = 2\pi$ and $e = 0.1, 0.3, 0.5, 0.7, 0.9$. Left: σ of errors for the passage **time** through pericenter. Right: σ of errors in **energy**. Both has a function of **number of revolutions**. Everything in $\log_{10}$ scales. **Slopes:** $\approx 3/2$, $\approx 1/2$, respectively. Taylor used to order 28 and truncation error set to 10^{-22}. 100 runs. Computing time: 140^{m} for $e = 0.1$, 558^{m} for $e = 0.9$. Note the **strange improved behaviour of** $e = 0.7$.

Hénon-Heiles system: non-integrable, both **regular and chaotic**

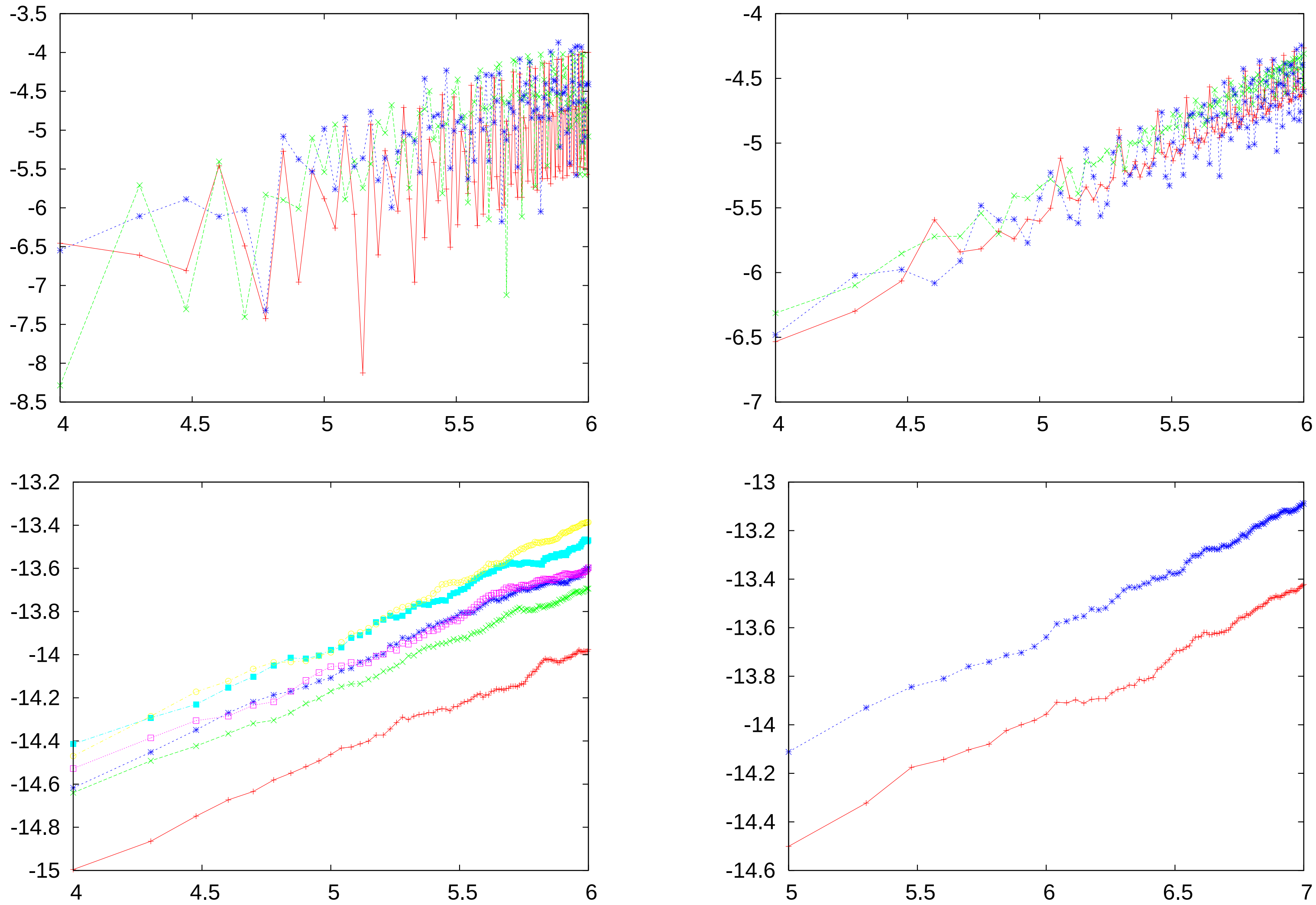

Horizontal axis: the number of Poincaré iterates.

Top left: σ for the **return time**.
Top right: σ for the **position errors**.
Energies: 0.050, 0.100, 0.125, **regular orbits**.
Respective **slopes:**$\approx 3/2, \ \approx 1$.

Bottom: σ for the **energy**. Both **regular orbits** (energies as before) and **chaotic** (energies 0.125, 0.166, 0.1666666666).
Right: larger number of Poincaré iterations.
Slope: $\approx 1/2$.

All data in $\log_{10}$ scales

Taylor to order 32 and truncation error 10^{-22}.

Similar behaviour for preservation of **energy and components of angular momentum** for the **Sun-Jupiter-Saturn-Uranus-Neptune** for 4.5×10^9 **years**. **Maximal error** $< 10^{-10}$, or $\approx 10^{-11}$ as relative error.

Some applications

Just to name a few:

- Computation of Poincaré maps, variational and higher variational equations, periodic orbits, invariant tori, invariant manifolds, homo and heteroclinic connections in relatively simple models, requiring a good accuracy,
- Analysis of models depending on several parameters, looking for bifurcations, Lyapunov exponents, rotation number, frequency analysis, etc, in massive simulations, where computing time is relevant,
- Problems where multiple precision is essential: splitting of separatrices for systems not far from integrable, detection of the order of regularity of some phenomena (e.g.: problems of regularisation),
- It has been applied to compute space missions, choreographies, etc.
- Use of Poincaré maps, Lyapunov exponents, frequency analysis, transversality of invariant manifolds, monodromy matrices and groups, and higher order extensions, to detect non-integrability in Hamiltonian systems.

Additional comments on Taylor method

Taylor method is **suitable and fast provided** the system to be integrated is analytic (or $\mathscr{C}^r$ with r big), with a r.h.s. which is not difficult to evaluate explicitly.

With some **caution** in the selection of order and truncation error can be **as accurate as possible**, the main source of error being round off errors.

It seems to be **unbeatable** when faced to **multiprecision**.

It is **not suitable** for **stiff systems, systems for which the evaluation of the vector field has to be done by indirect methods (as in some evolution PDE) or for systems whose solutions pass close to singularities which occur for complex time with small imaginary part**.

Stability of the triangular points in the circular 3D RTBP (Work in progress)

Known results

- They are linearly stable for the mass parameter $\mu \in [0, \mu_1]$, where

$$\mu_s = \omega_{\text{short}}/\omega_{\text{long}} = s, \qquad s \in \mathbb{N}.$$

$\omega_{\text{short}}, \omega_{\text{long}}$ = frequencies at $L_{4,5}$ in the 2D case. $\omega_z = 1$.

$$\left[(1 \pm (1 - 27\mu(1-\mu))^{1/2})/2\right]^{1/2}.$$

- Nonlinear stability for $\mu \in [0, \mu_1] \setminus \{\mu_2, \mu_3\}$ in the 2D case.
- The nonlinear stability of the spatial problem is unknown. Probably there is some amount of Arnol'd diffusion.
- There is a domain of "practical stability", around $L_{4,5}$, which is not too small.

Let $H = H_2 + H_3 + \ldots$ be the Hamiltonian around $L_{4,5}$.

$$H_2 = \frac{1}{2}\omega_s(q_1^2 + p_1^2) - \frac{1}{2}\omega_l(q_2^2 + p_2^2) + \frac{1}{2}\omega_z(q_3^2 + p_3^2).$$

Compute NF up to a suitable order, assuming no resonance. Bound the remainder and its effect $|\dot{I}_j|$ on actions of the NF. Use linear combinations of the actions which define a convex set around the triangular points.

Given T and δ, there exists an initial radius, ρ_0, such that if $(Q, P)_{t=0} \in B_{\rho_0}$ then $(Q, P)_t \in B_{\rho_0(1+\delta)}$ for all $|t| < T$, where B_ρ denotes the ball of radius ρ centered at the origin. I.e. **practical or effective stability**.

As a result one obtains, in general, **explicit Nekhorosev type estimates** (i.e., for δ fixed, one has $T \approx \exp(c/\rho^d)$, for some positive constants c, d).

- Numerical simulations show a **large "stable domain"**.

The stability domain

Conditions to be satisfied:

a) Projection on (x, y) **not encircling the main primary**,

b) Not **too close approaches to primaries**,

c) Projection on (x, y) **not below some critical** y (e.g. $y_c = -0.5$).

d) Starting on **zero velocity surface**.

On the integration method

Integration of ODE is done using a **Taylor method**.

Numerical values of the coefficients computed by recurrence (automatic differentiation formulae) up to high order (e.g. order 24) and with time step such that the requested local error is below the ε of the processor (e.g. 10^{-21}).

Question What about **energy conservation**?

Long range integrations for the 3D RTBP

For $\mu = 0.001$ a test on a sample of 175 i. c. as follows has been done: $\Delta\rho = -0.001\,(0.0005)\,0.001;\ \ \alpha = 0.1\,(0.05)\,0.4;\ \ z = 0\,(0.2)\,0.8$, heliocentric, from a suitable origin of $\rho = R - 1$, α in revolutions. 75 points subsist for $t_{\text{final}} = 10^9$ Jupiter revolutions ($\approx$ **twice the age of Solar System**).

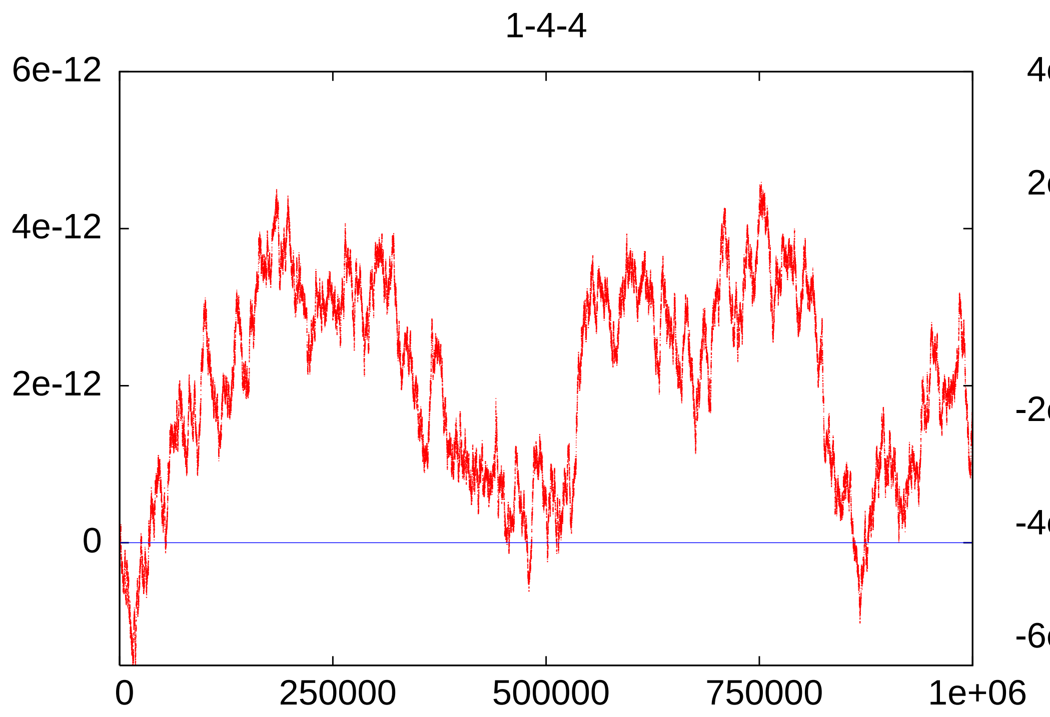

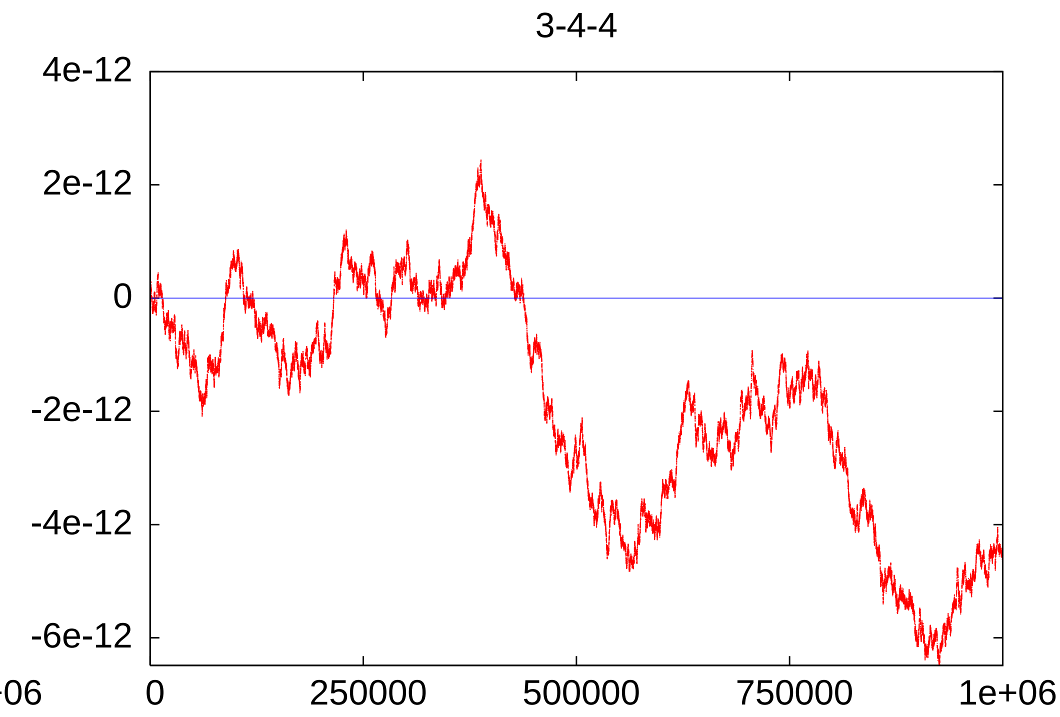

Shown: the 3 worst cases and the best one.

Errors w.r.t. initial energy displayed every 1000 Jupiter revolutions (J.r.).

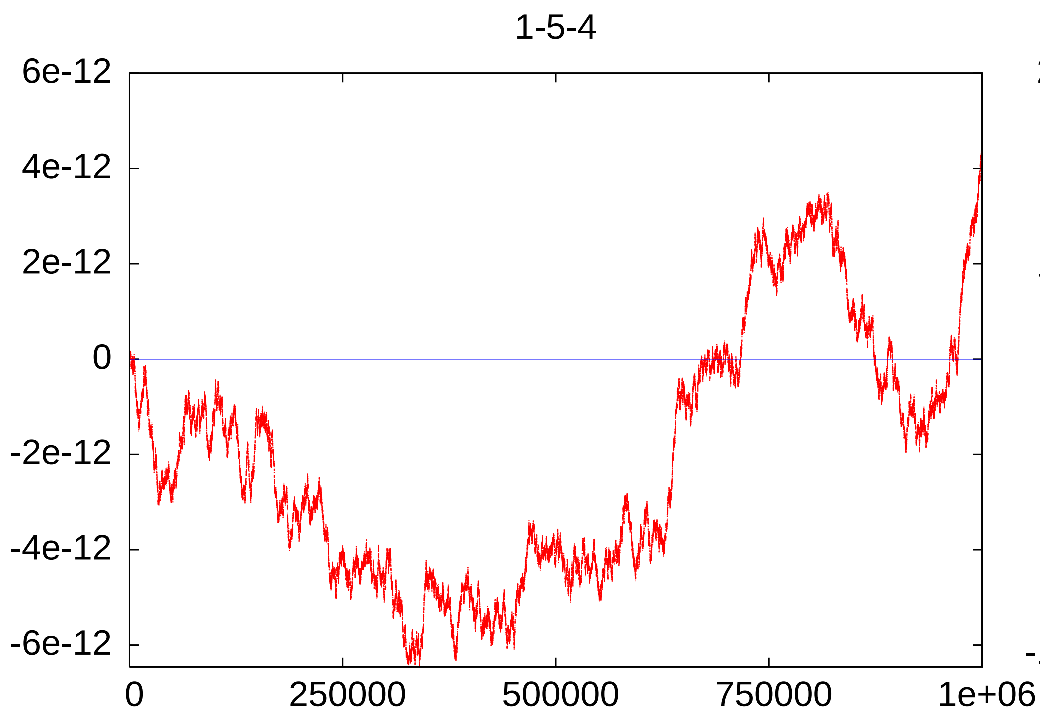

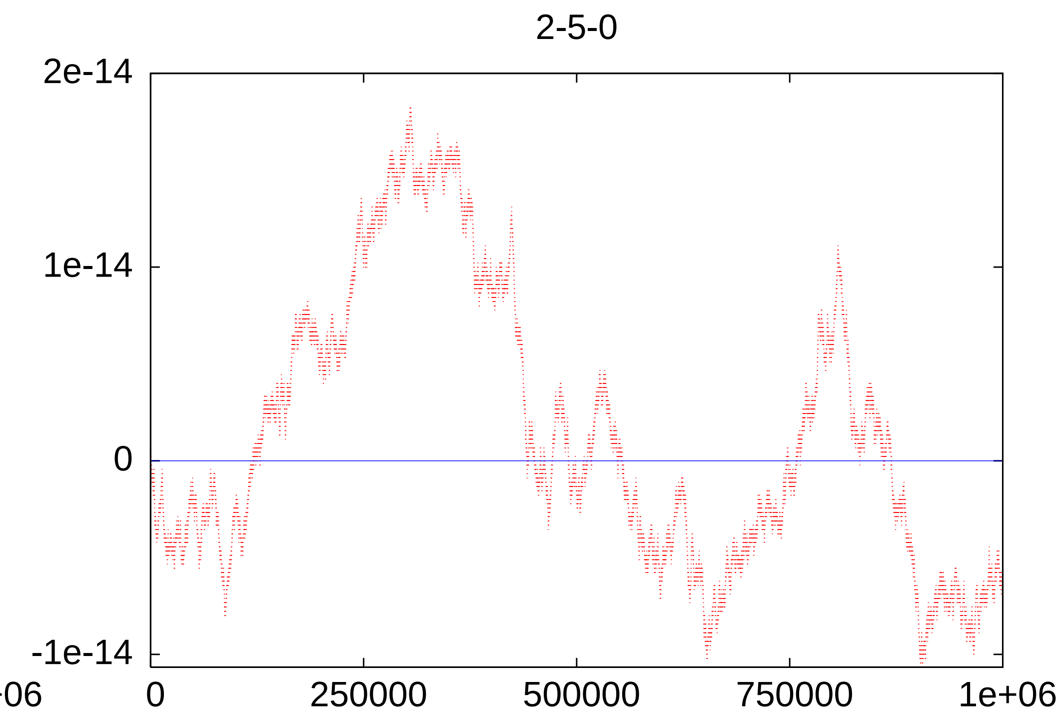

Average **integration step**: Worst case 0.36 years; best case 2.08 years.

Relevant statistics:

a) Histogram of **jumps of energy** every 1000 J.r. Unit: $2^{-52} \approx 2 \times 10^{-16}$,

b) **Maximal errors** and $1\,\sigma$ predicted values from previous plots,

c) **Autocorrelation** for the worst case.

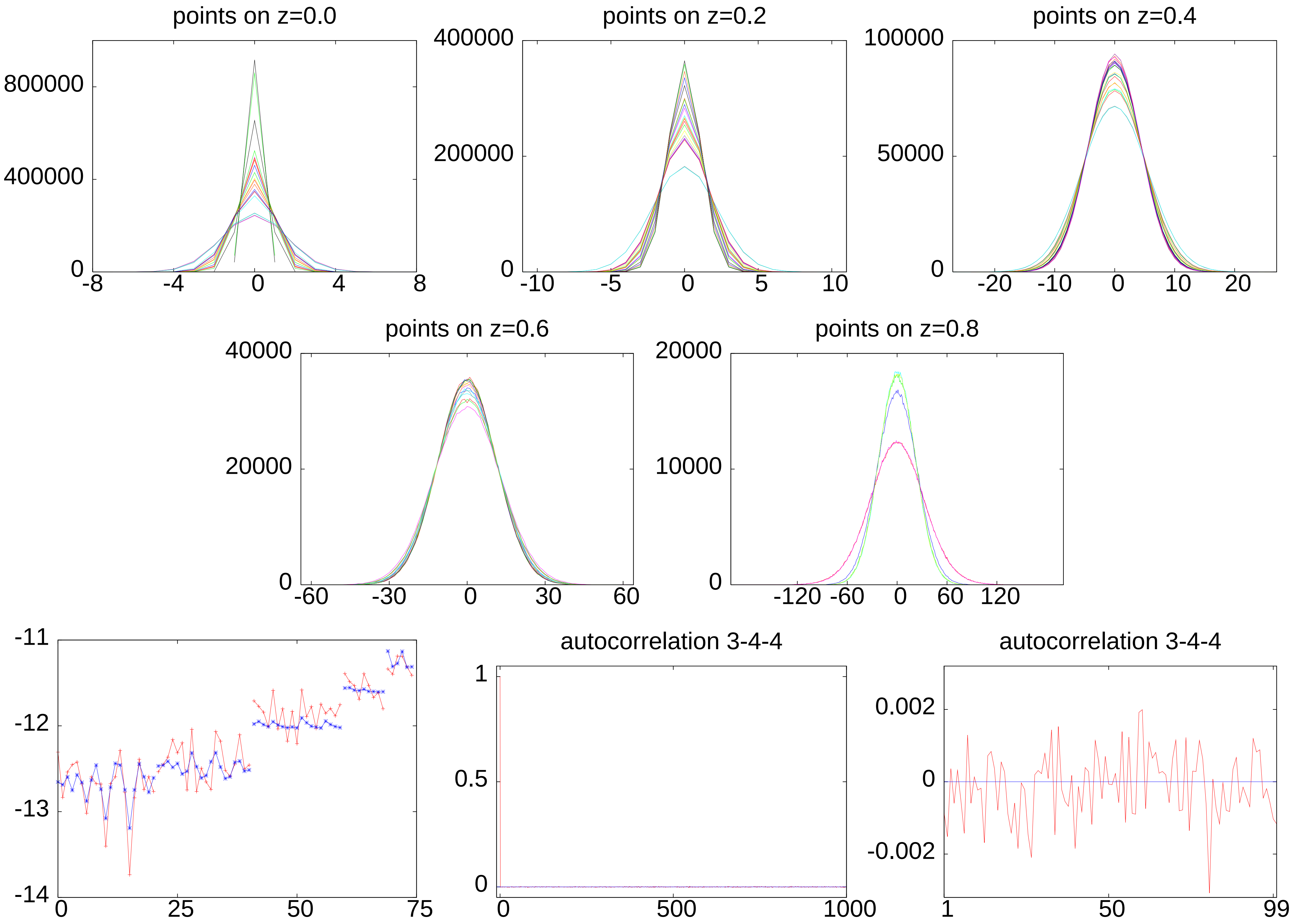
points on z=0.0
800000
400000
0
-8
-4
0
4
8
points on z=0.2
400000
200000
0
-10
-5
0
5
10
points on z=0.4
100000
50000
0
-20
-10
0
10
20
points on z=0.6
40000
20000
0
-60
-30
0
30
60
points on z=0.8
20000
10000
0
-120
-60
0
60
120
-11
-12
-13
-14
0
25
50
75
autocorrelation 3-4-4
1
0.5
0
0
500
1000
autocorrelation 3-4-4
0.002
0
-0.002
1
50
99

Preliminary results: Statistics

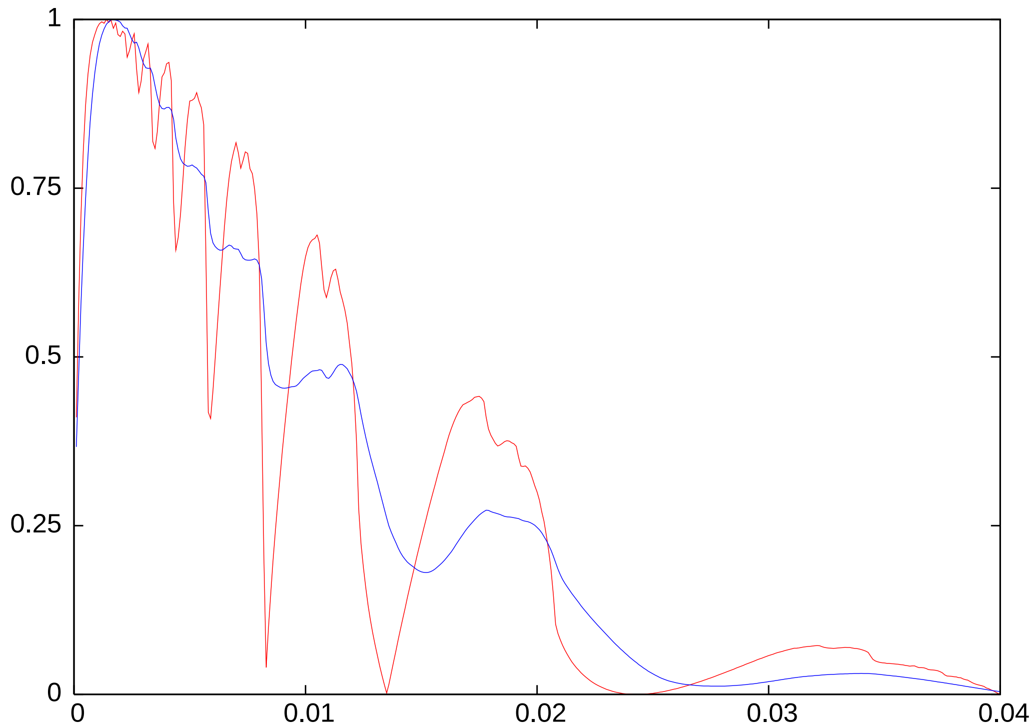

Normalized subsisting points. Planar case: $\Delta\rho = 10^{-4}$, $\Delta\alpha = 2 \times 10^{-4}$. Maximal value, for $\mu = 0.0014$, 282757 points. Spatial case: $\Delta\rho = 10^{-4}$, $\Delta\alpha = 5 \times 10^{-4}$, $\Delta z = 5 \times 10^{-3}$. Maximal value, for $\mu = 0.0017$, 19014882 points. Total scanned points: 8×10^{10}. Subsisting a first filter 2.17×10^{9}. The role of resonances is clearly seen (2D, 3D differ)

Spatial case refinement finished recently.

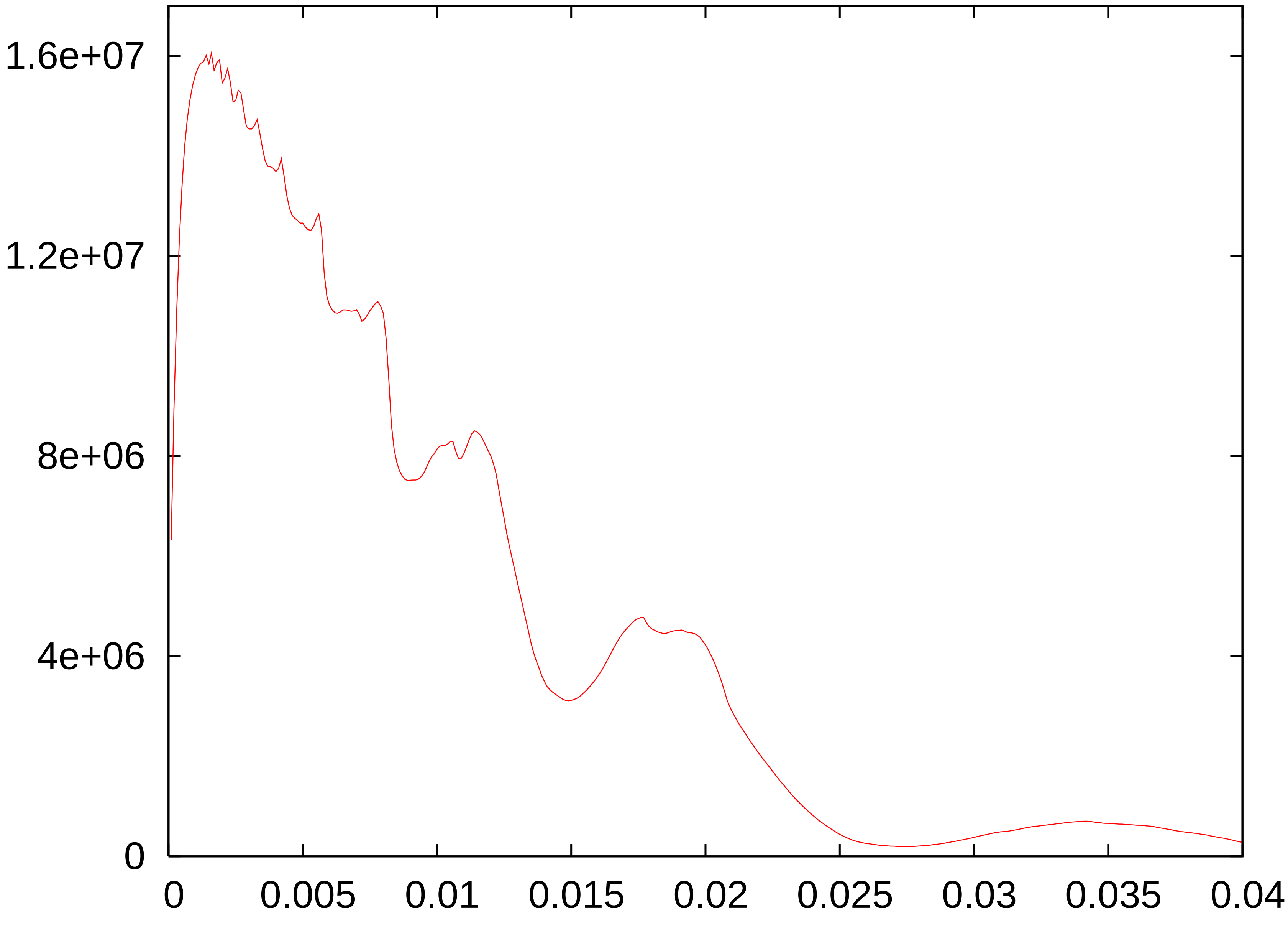
1.6e+07
1.2e+07
8e+06
4e+06
0
0
0.005
0.01
0.015
0.02
0.025
0.03
0.035
0.04

The case $\mu = 0$

For $\mu = 0$ one must be in $1-1$ resonance. Hence

$$z = \sqrt{\frac{4}{(1+R^2)^2} - R^2},$$

or

$$\psi = 1 - \frac{1}{2}w + \frac{3}{2^5}w^2 - \frac{1}{2^8}w^3 - \frac{25}{2^{13}}w^4 + \frac{33}{2^{16}}w^5 + \frac{175}{2^{20}}w^6 - \frac{497}{2^{23}}w^7 - \frac{4401}{2^{29}}w^8 + O(w^9),$$

where $w = z^2$, $\psi = \psi(z) = R^2$.

This suggests to plot $(\alpha,\ 1+\rho-\sqrt{\psi(z)},\ z)$.

Variables used for the representations: Cylindrical Heliocentric, with α in revolutions, $\rho = r_1 - 1$, z.

A sample of results

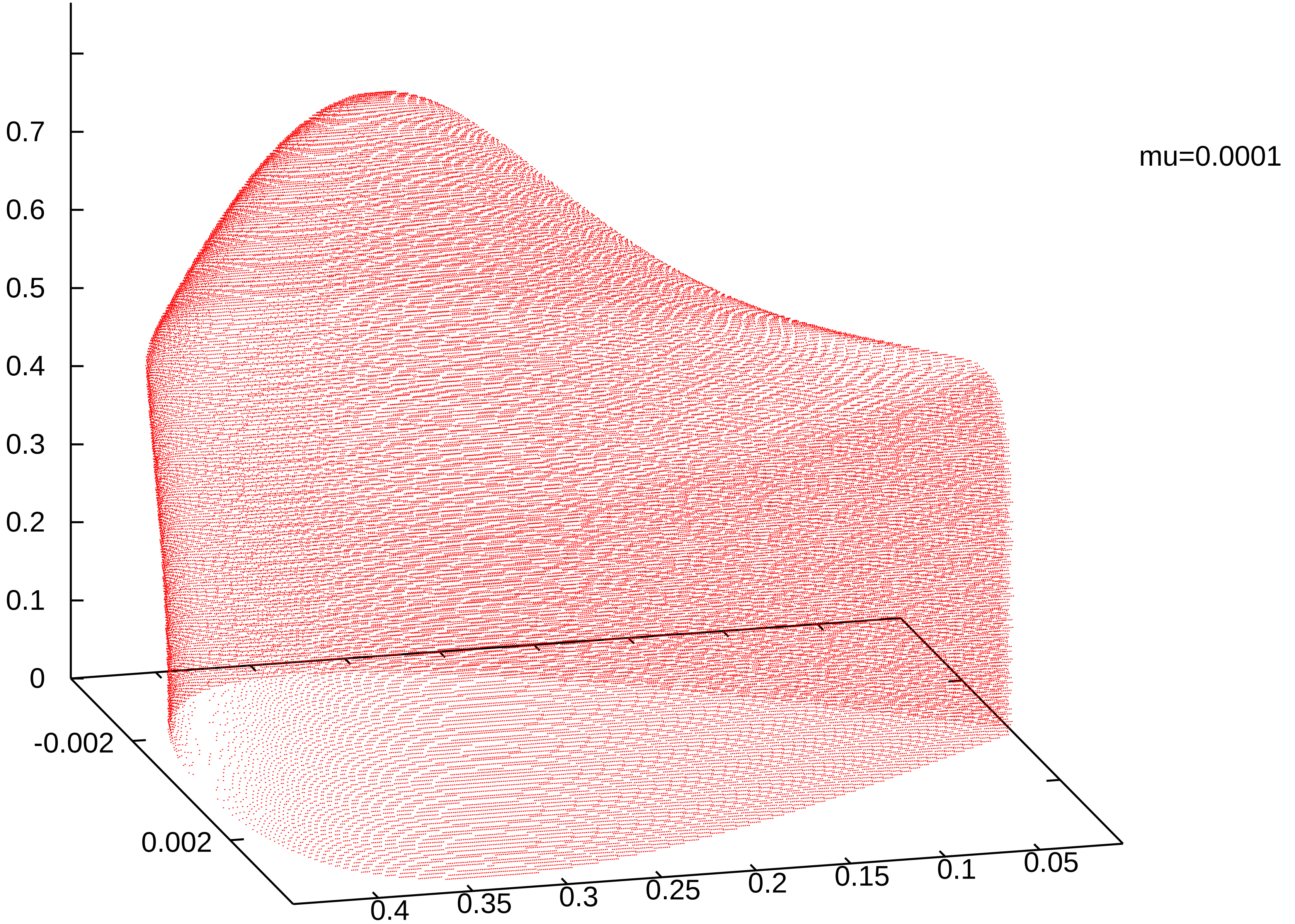

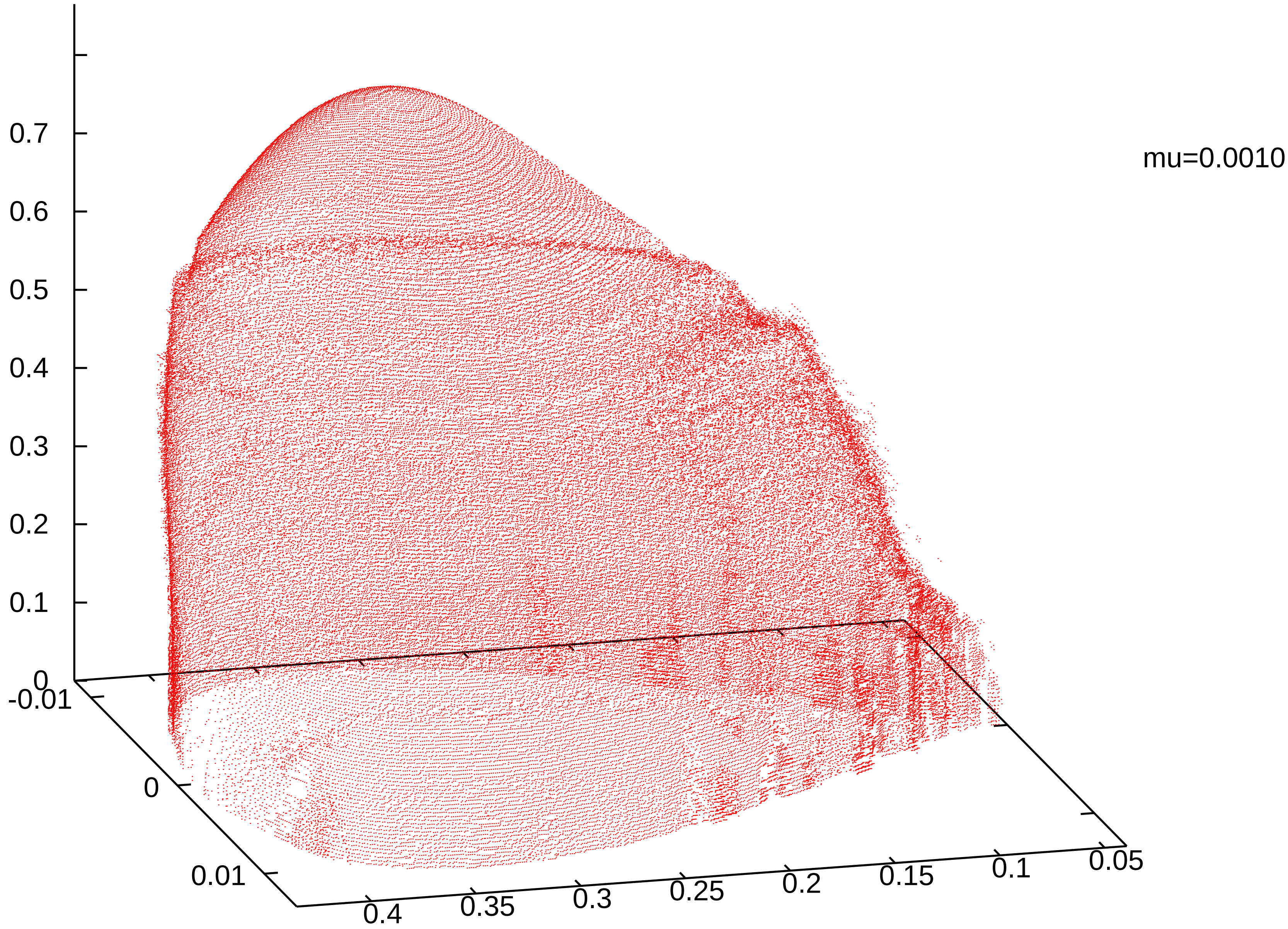

mu=0.0010
0.7
0.6
0.5
0.4
0.3
0.2
0.1
0
-0.01
0
0.01
0.4
0.35
0.3
0.25
0.2
0.15
0.1
0.05

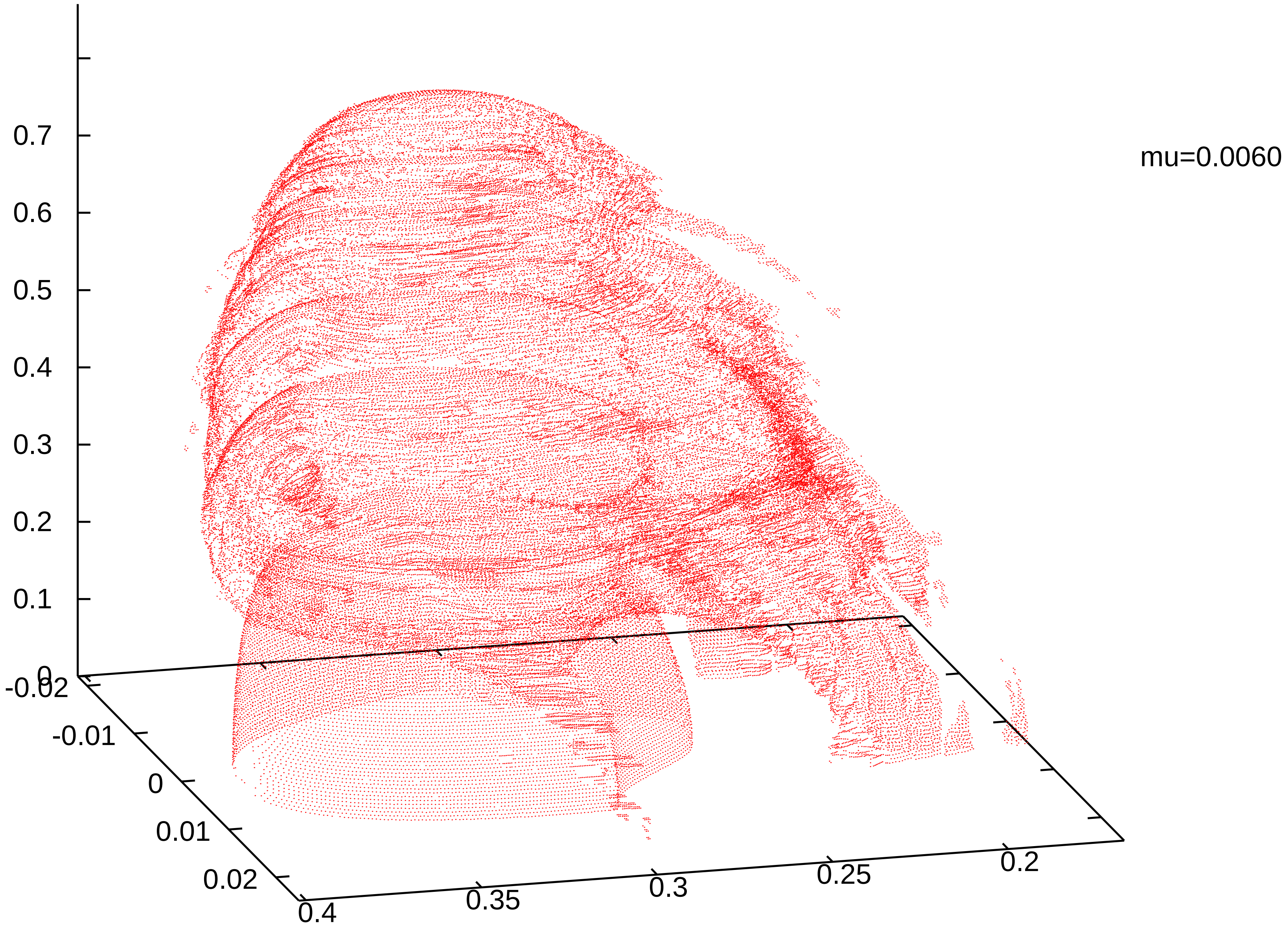

mu=0.0060
0.7
0.6
0.5
0.4
0.3
0.2
0.1
0
-0.02
-0.01
0
0.01
0.02
0.4
0.35
0.3
0.25
0.2

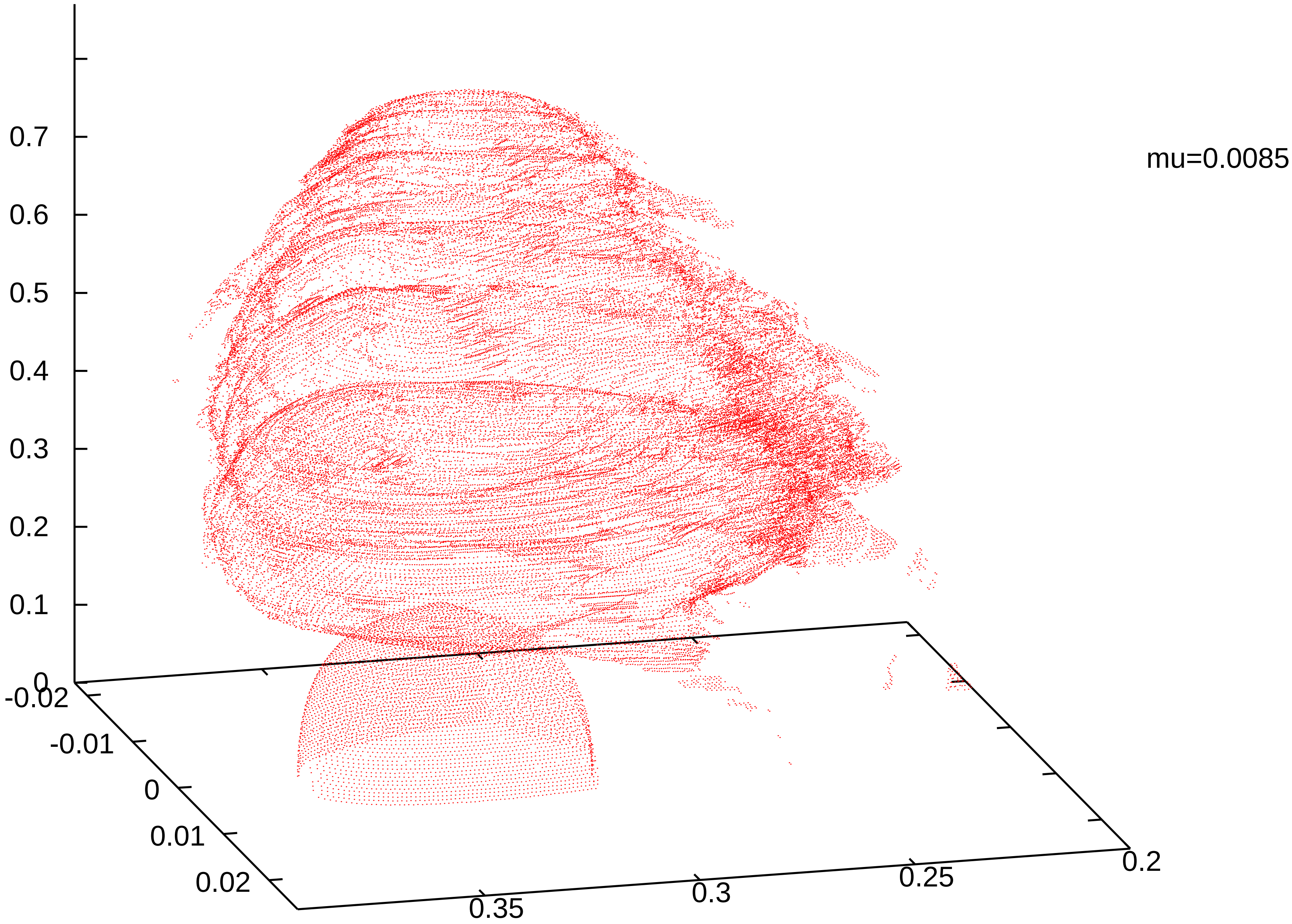

mu=0.0085
0.7
0.6
0.5
0.4
0.3
0.2
0.1
0
-0.02
-0.01
0
0.01
0.02
0.35
0.3
0.25
0.2

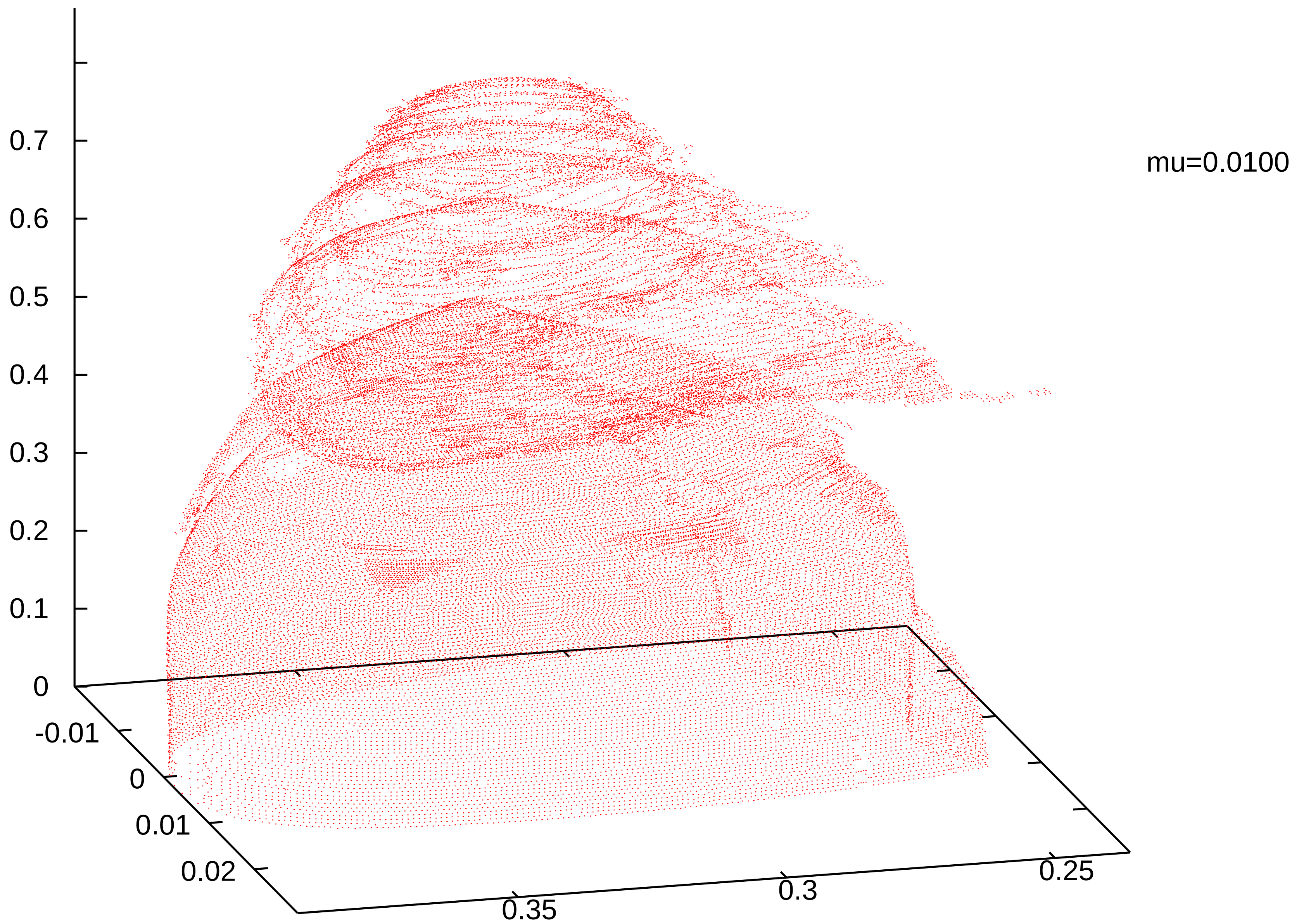

mu=0.0100
0.7
0.6
0.5
0.4
0.3
0.2
0.1
0
-0.01
0
0.01
0.02
0.35
0.3
0.25

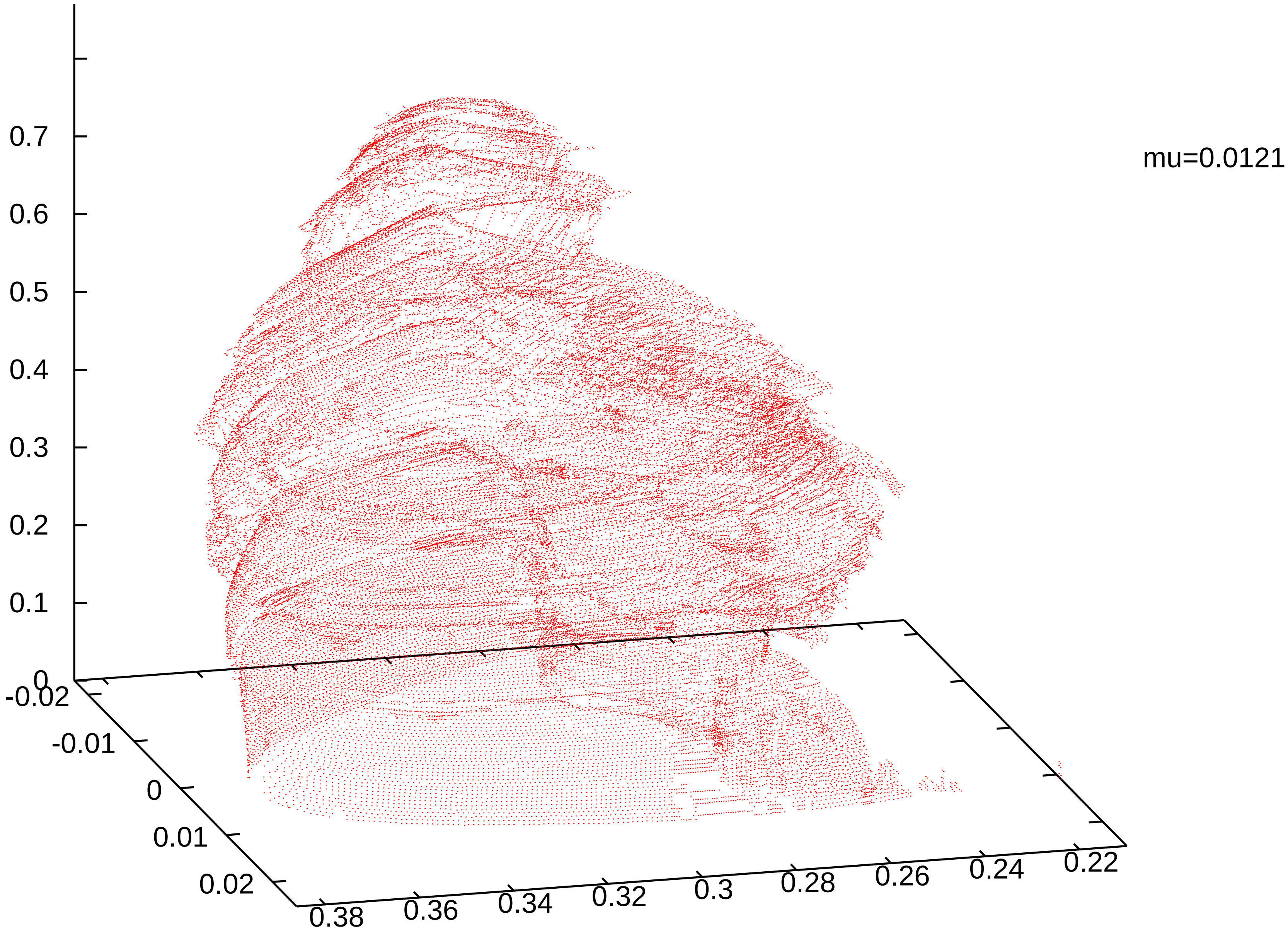

0.7
0.6
0.5
0.4
0.3
0.2
0.1
0
-0.02
-0.01
0
0.01
0.02
0.38
0.36
0.34
0.32
0.3
0.28
0.26
0.24
0.22
mu=0.0121

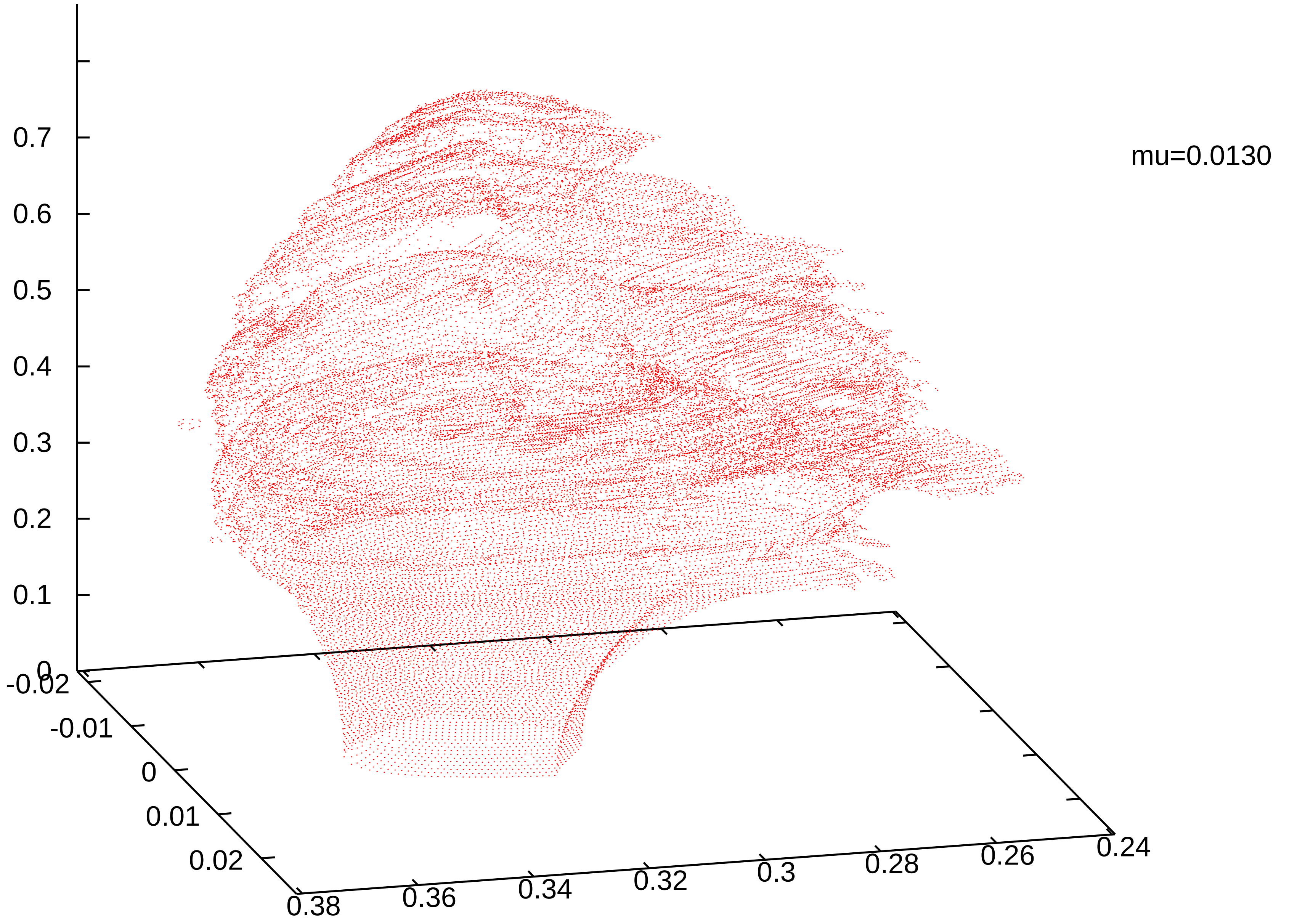

mu=0.0130
0.7
0.6
0.5
0.4
0.3
0.2
0.1
0
-0.02
-0.01
0
0.01
0.02
0.38
0.36
0.34
0.32
0.3
0.28
0.26
0.24

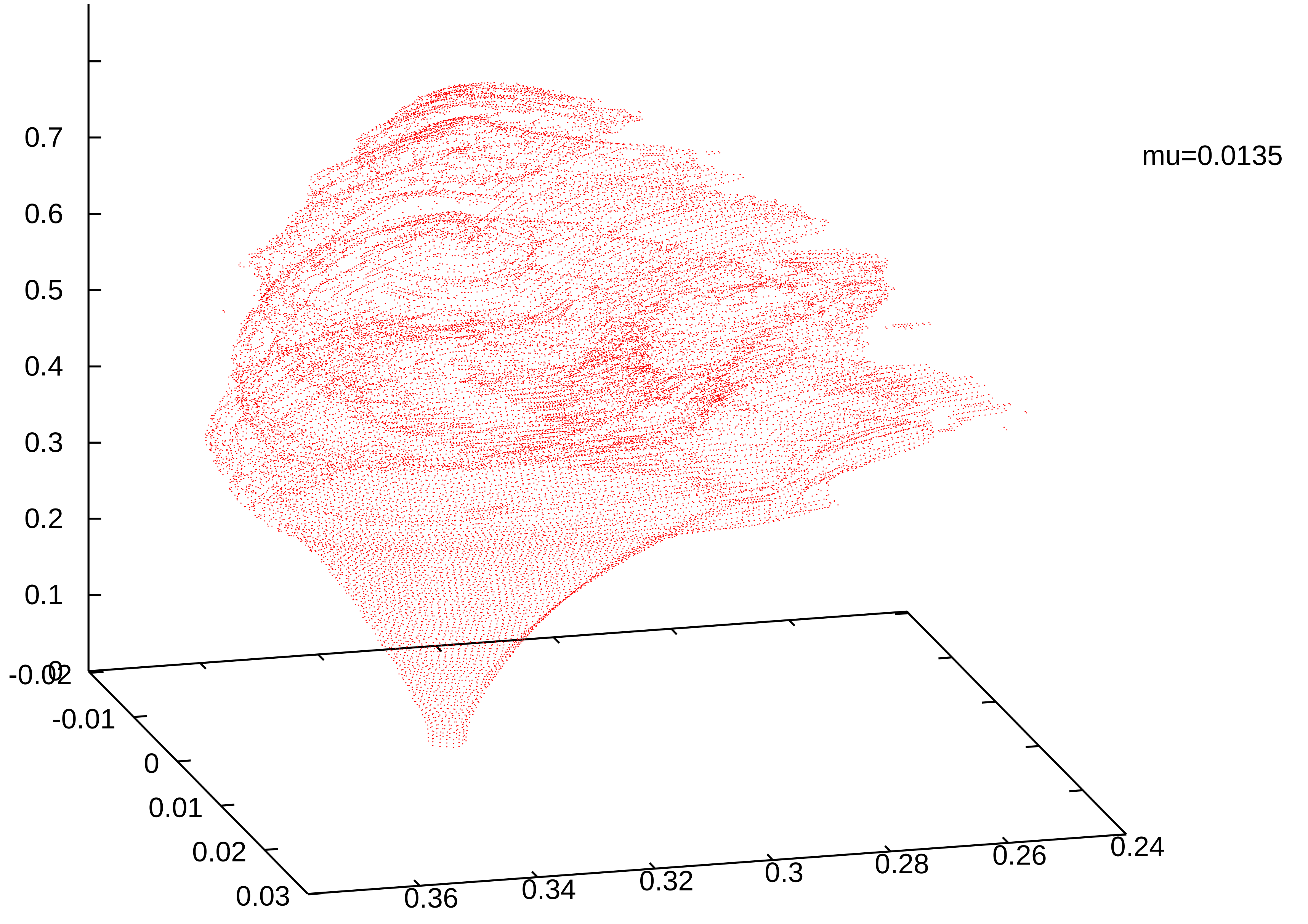
mu=0.0135
0.7
0.6
0.5
0.4
0.3
0.2
0.1
0
-0.02
-0.01
0
0.01
0.02
0.03
0.36
0.34
0.32
0.3
0.28
0.26
0.24

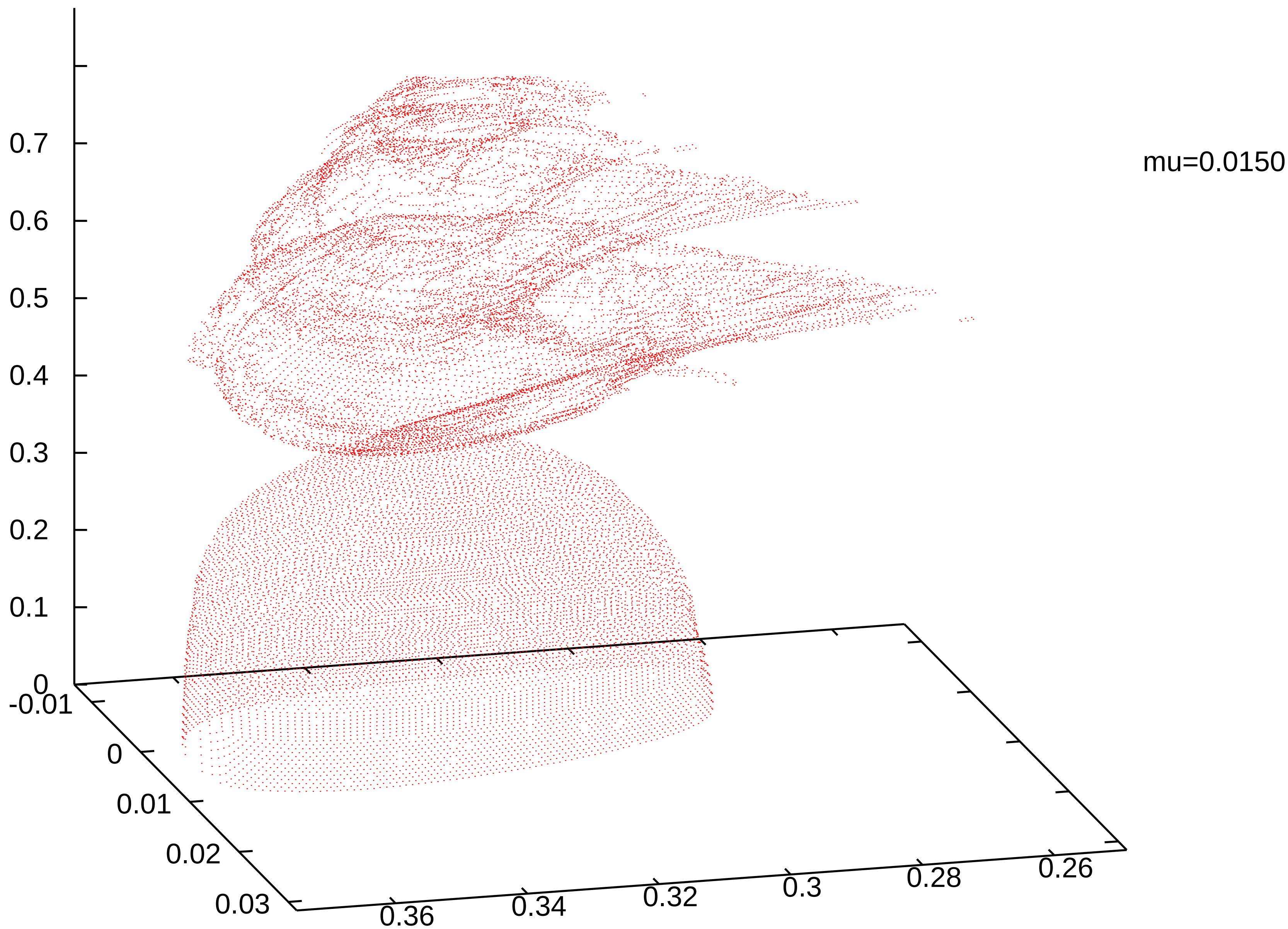

mu=0.0150
0.7
0.6
0.5
0.4
0.3
0.2
0.1
0
-0.01
0
0.01
0.02
0.03
0.36
0.34
0.32
0.3
0.28
0.26

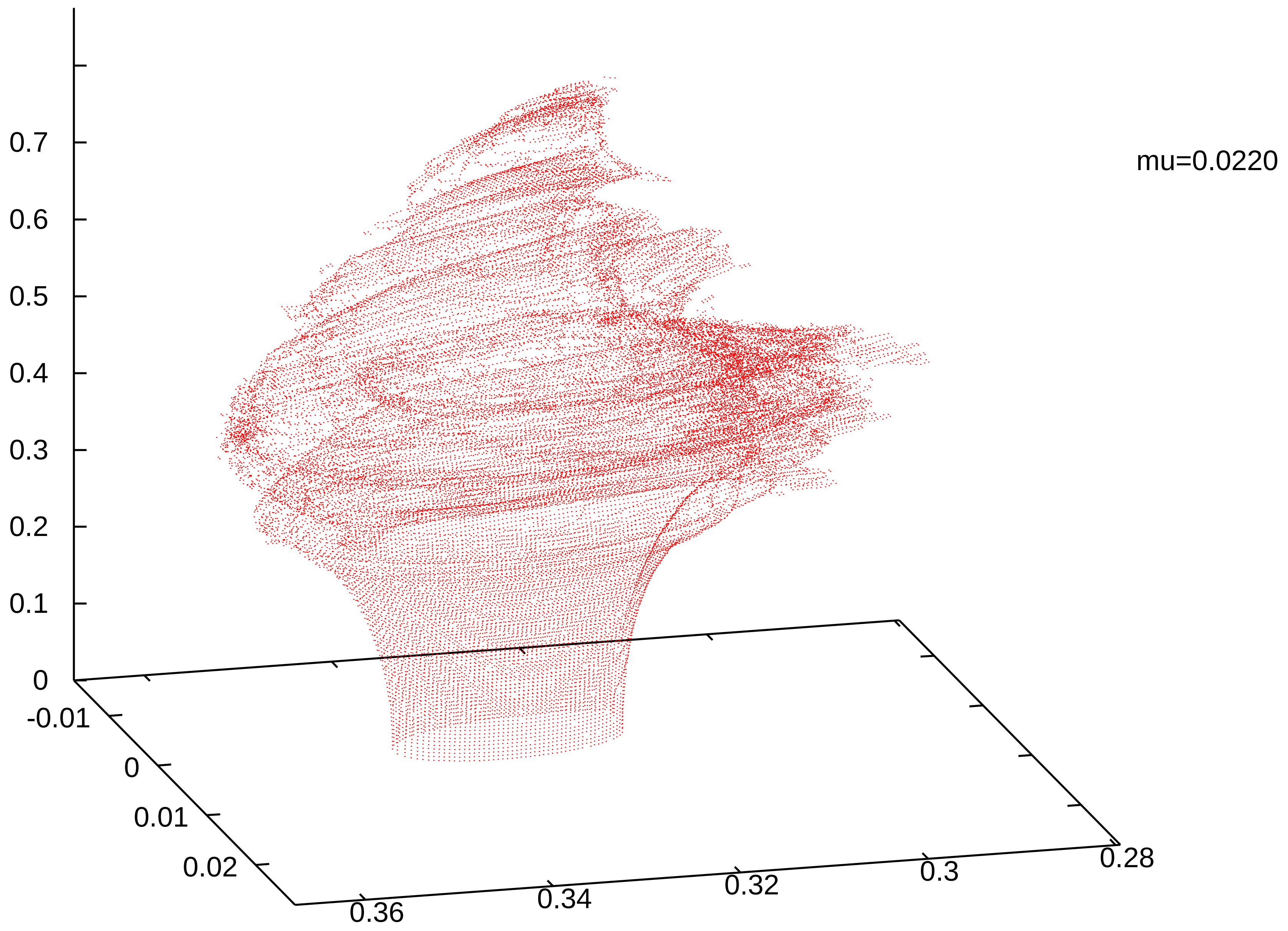

mu=0.0220
0.7
0.6
0.5
0.4
0.3
0.2
0.1
0
-0.01
0
0.01
0.02
0.36
0.34
0.32
0.3
0.28

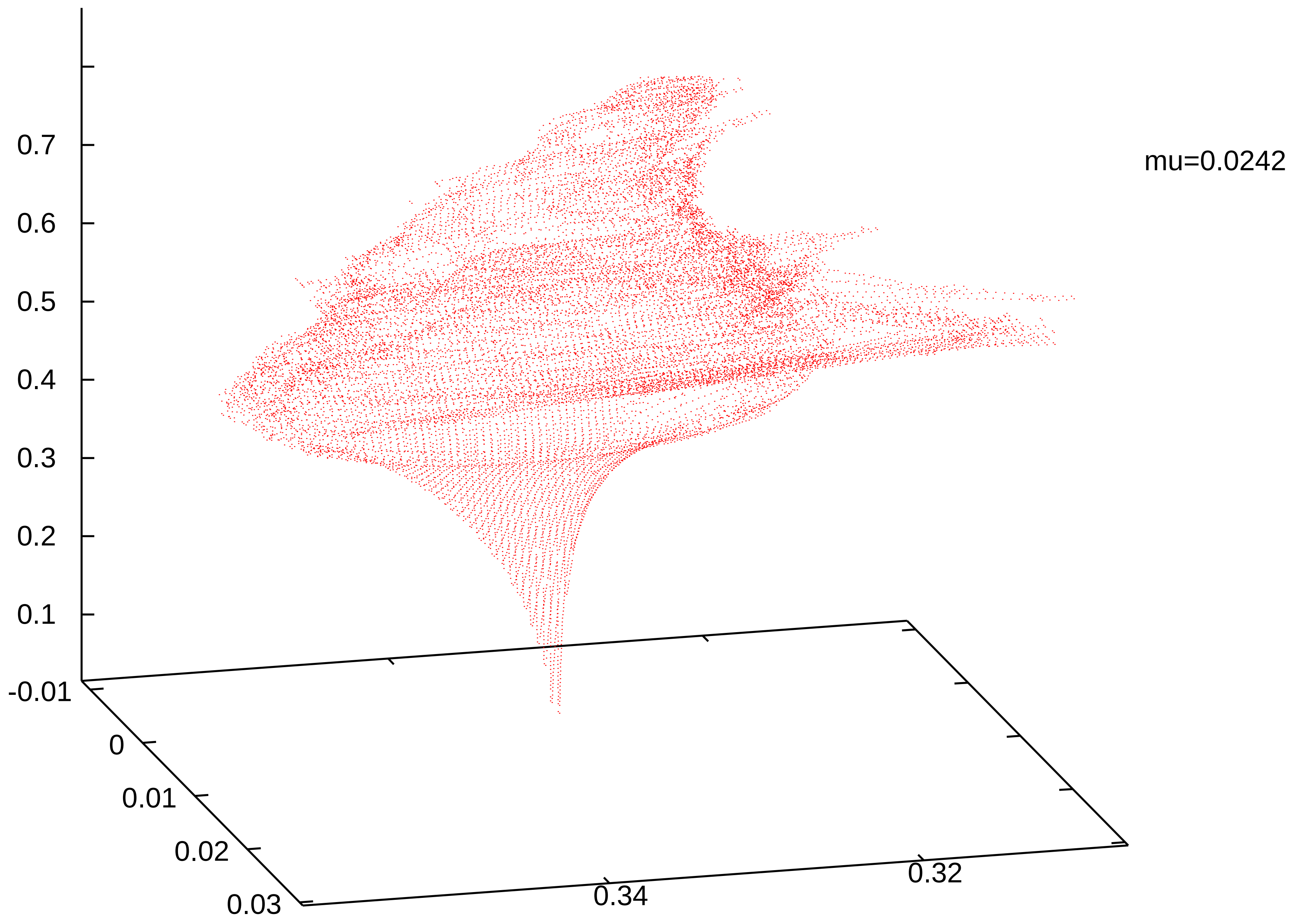
0.7
0.6
0.5
0.4
0.3
0.2
0.1
-0.01
0
0.01
0.02
0.03
0.34
0.32
mu=0.0242

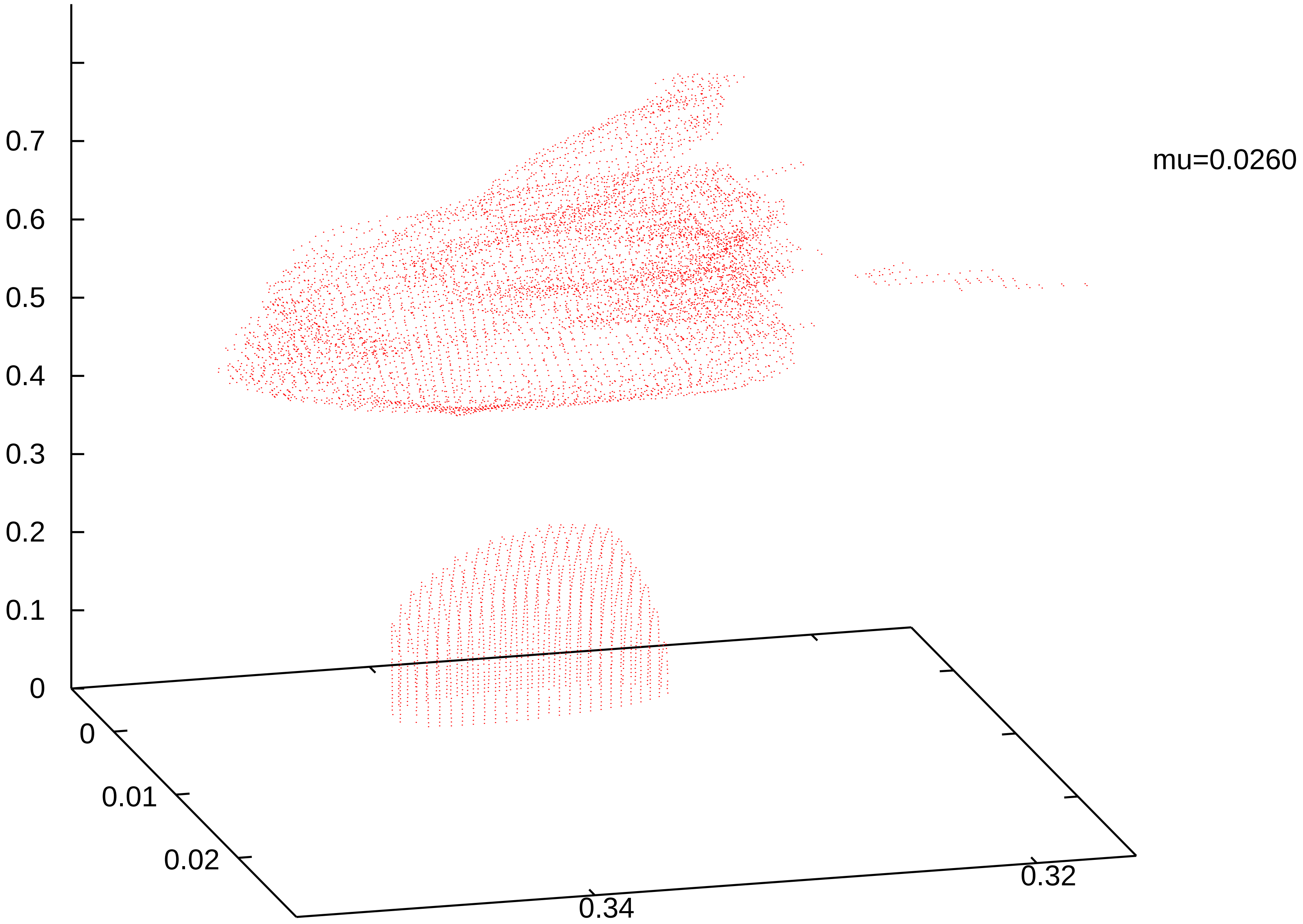

mu=0.0260
0.7
0.6
0.5
0.4
0.3
0.2
0.1
0
0
0.01
0.02
0.34
0.32

Next task is the identification of the different objects which "bound" (in some way) those regions of "numerical practical stability". In general this task becomes increasingly difficult when increasing μ. However some parts of the boundaries are associated to sharp transitions : nearby points escape quickly or remain on the desired region for very long time. In this case the identification becomes easier.

For the moment some of these object are identified as union of stable/unstable manifolds of invariant (normally hyperbolic) tori sitting on the center manifold of the collinear point L_3 or on the center manifold of families of periodic orbits of elliptic-hyperbolic type. The type of a periodic orbit can be seen in any Poincaré section.

All of these objects are codimension 1 and play a key role in many applied sciences.

Still **a lot of work** to be done ...

Other applications

Just to name a few:

- Computation of periodic orbits, invariant tori, invariant manifolds, homo and heteroclinic connections in relatively simple models, requiring a good accuracy,
- Analysis of models depending on several parameters, looking for bifurcations, Lyapunov exponents, in massive simulations, where computing time is relevant,
- Problems where multiple precision is essential: splitting of separatrices for systems not far from integrable, detection of the order of regularity of some phenomena (e.g.: problems of regularisation),
- It has been applied to compute space missions, choreographies, etc.

Final comments

Taylor method is suitable and fast provided the system to be integrated is analytic (or $\mathscr{C}^r$ with r big), with a r.h.s. which is not difficult to evaluate explicitly.

With some caution in the selection of order and truncation error can be as accurate as possible, the main source of error being round off errors.

It seems to be unbeatable when faced to multiprecision.

It is not suitable for stiff systems, systems for which the evaluation of the vector field has to be done by indirect methods (as in some evolution PDE) or for systems whose solutions pass close to singularities which occur for complex time with small imaginary part.